



This is a repository copy of *Quantitative review of probabilistic approaches to fatigue design in the medium cycle fatigue regime*.

White Rose Research Online URL for this paper:

<https://eprints.whiterose.ac.uk/209423/>

Version: Published Version

Article:

Kufoin, E. and Susmel, L. orcid.org/0000-0001-7753-9176 (2024) Quantitative review of probabilistic approaches to fatigue design in the medium cycle fatigue regime. *Probabilistic Engineering Mechanics*, 75. 103589. ISSN 0266-8920

<https://doi.org/10.1016/j.probengmech.2024.103589>

Reuse

This article is distributed under the terms of the Creative Commons Attribution (CC BY) licence. This licence allows you to distribute, remix, tweak, and build upon the work, even commercially, as long as you credit the authors for the original work. More information and the full terms of the licence here:

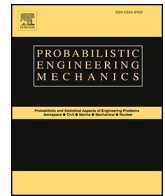
<https://creativecommons.org/licenses/>

Takedown

If you consider content in White Rose Research Online to be in breach of UK law, please notify us by emailing eprints@whiterose.ac.uk including the URL of the record and the reason for the withdrawal request.



eprints@whiterose.ac.uk
<https://eprints.whiterose.ac.uk/>



Quantitative review of probabilistic approaches to fatigue design in the medium cycle fatigue regime

Elvis Kufoin, Luca Susmel*

Department of Civil and Structural Engineering, The University of Sheffield, Mappin Street, Sheffield, S1 3JD, UK

ARTICLE INFO

Keywords:

Medium cycle fatigue
Scatter band
Probability of survival
Regression analyses
Stress levels
Fatigue design

ABSTRACT

To quantify the fatigue behaviour of materials, a Wöhler diagram is required. The state of the art shows that, over the years, numerous approaches suitable for determining Wöhler curves have been devised and validated through large fatigue data sets. The variation in experimental fatigue data elicits the use of statistics for analysis and design purposes. By focusing on the medium-cycle fatigue regime (i.e., failures in the range 10^3 – 10^7 cycles to failure), this paper reviews relevant statistical approaches, particularly the methods suggested by the American Society for Testing Materials (ASTM) as well as the International Institute of Welding (IIW) and the so-called Linear Regression Method (LRM). Their responses were assessed on virtual data sets tailored to satisfy specific statistical requirements as well as experimental fatigue data sets from the literature. While the scatter bands at two times or less of the spread are similar for all approaches, the ASTM approach is seen to be the most conservative.

1. Introduction

To guarantee the structural integrity of components during in-service operations, fatigue design considerations are a key aspect to address because repeated cyclic loading accounts for most failures [1]. Factors accounting for crack initiation range from material microstructure, loading path, geometry, defects and environment [2]. Designing against fatigue, therefore, becomes complex when considering these factors. A stress (S) – number of cycles to failure (N) curve (i.e., the so-called "Wöhler curve" or "S–N curve") summarises the failure ratio and has shapes that depend on both the trend in the experimental result and methods used to model the curve [3]. Before progressing, it is important to briefly explain how an S–N curve is generated.

The S–N curve, also referred to as the Wöhler curve, is a graphic representation of the relationship between applied stress and the corresponding number of cycles to failure for a material under specific loading conditions and the environment. Fatigue data comprises of a stress level (σ), wherein σ can be the stress amplitude, maximum stress in the cycle, or stress range, alongside the number of cycles (N_f) the material endures before failure. By subjecting numerous specimens to various stress levels (σ_i , $i = 1..n$, with n being the total number of specimens), an experimental dataset ($\sigma_i, N_{f,i}$) is obtained, which in turn is utilized to construct the S–N curve. Fig. 1 illustrates the profile of an

S–N curve particularly in the medium cycle fatigue (MCF) regime where (for the sake of clarity) the curve is assumed to be linear in the log – log space. The shapes of the curve in the low cycle fatigue (LCF) and high cycle fatigue (HCF) regimes are dependent on the material. Of particular interest is the shape of the curve in the HCF, which is horizontal if the material has a fatigue limit σ_0 . The fatigue limit is the theoretical stress level below which failure does not occur. For materials that do not have a fatigue limit, an endurance limit is estimated at a referenced number of cycles, typically in the region of 10^6 and 10^8 cycles, and the curve continues with the same gradient beyond this point. In some cases, the fatigue curve deviates in steepness from the one that describes the medium-cycle fatigue behaviour of the same material, resulting in the observation of a knee point. Beyond the HCF is the very high cycle fatigue (VHCF) regime typically occurring beyond approximately 10^7 cycles. The shape of the curve in this region depends on the material. Some materials may exhibit a fatigue limit within this region, leading to the observation of a second horizontal plateau in the S–N curve.

The S–N curve in the LCF is either modelled in accordance with Coffin–Manson and Morrow model [4] or, under some stated considerations, the ASTM strain-energy approach [5]. A Weibull model can also be used as explained in Ref. [6]. The behaviour in the MCF regime can be modelled using stress-based approaches like in linear regression analysis or by using the Basquin approach. Similar to the LCF, the Coffin–Manson strain-based approach can also be used in the MCF region. These

* Corresponding author.

E-mail address: l.susmel@sheffield.ac.uk (L. Susmel).

Nomenclature

C_0	Intercept of mean S–N curve (constant)
C_1	Coefficient of independent variable (constant)
k	Negative inverse slope
$K_{D(Owen)}$	Scatter factor from Owen tolerance limit approach
$K_{D(LM)}$	Scatter factor from the linear regression approach
$K_{D(ASTM)}$	Scatter factor from the ASTM approach
K_D	Scatter factor
$\log N_{f,ij}$	Log of life at the replication level
$\overline{\log N_{fij}}$	Mean log of life at the replication level
$\overline{\log \sigma_i}$	Mean log of stress level, $\overline{\log \sigma_i} = \sum_{i=1}^n \frac{\log \sigma_i}{n}$
$\overline{\log N_{f,i}}$	Mean log of fatigue life, $\overline{\log N_{f,i}} = \sum_{i=1}^n \frac{\log N_{f,i}}{n}$
$\log N_{f,D}$	Log of estimated life for design life
m_i	Replication level at the i th stress level
N_f	Number of cycles to failure
$N_{f,i}$	Number of cycles to failure at the i -th stress level

n	Number of experimental results (sample set)
n_σ	Number of stress levels
N_A	Reference number of cycles to failure
N_{kp}	Number of cycles to failure at the knee point
P_s	Probability of survival
q	Index depending on the probability of survival
R	Stress ratio ($R = \sigma_{\min}/\sigma_{\max}$)
s	Standard deviation of log cycles to failure
σ	Generic stress level (stress amplitude, maximum stress or stress range)
σ_i	i -th stress level ($i = 1, 2, \dots, n$)
$\sigma_{\min}, \sigma_{\max}$	Minimum and maximum stress in the cycle
σ_0	Endurance limit
$\sigma_{0,P\%}$	Endurance limit at a probability of survival P
$\sigma_{0,(1-P)\%}$	Endurance limit in error at a probability of survival P
T_σ	Scatter ratio of reference stress for $(1-P)\%$ and $P\%$ probabilities of survival
$\mu_{Y/X}$	Expected value of $\log N$ given $\log \sigma$

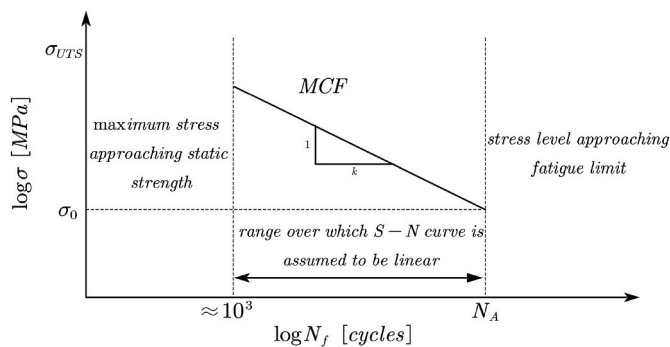


Fig. 1. S–N curve profile for the various fatigue regimes.

approaches can be extended to the HCF regime where the plastic contribution to the fatigue properties is insignificant. In the VHCF region, the assumptions behind the application on models in the LCF to HCF may not hold due to the increase in experimental scatter for decreasing stress amplitudes. Weibull and extreme value statistics are approaches that can be used to model the S–N curve in this region [2,7,8]. Different approaches can also be used, depending on the specific application. This paper will explore a few approaches used to model the S–N in the MCF regime.

Consider for example, the S–N curve in the MCF regime for practical design, where the variability in fatigue life results from various sources. Some of these sources include material mechanical properties, discontinuities, environmental factors and setup or equipment variations. This elicits for accurate analysis for design purposes. Cutting edge statistical approaches are commonly applied throughout the industry to post process experimental fatigue data. For instance, in Ref. [9] a Weibull Probabilistic Technique is used to estimate parameters, followed by a Bootstrap method for critical design. Similarly, Ref. [10,11] uses neural networks (NN) machine language for fatigue design, with neither the Weibull Probabilistic Technique nor NN assuming a distribution in the fatigue data. Though this has been successful, the statistical analysis of fatigue data remains tricky because the stress vs. fatigue life relationship is fundamentally nonlinear and the fatigue life distribution is assumed [5,12]. Other challenges originate from sample size which is restricted by cost and time, as well as varied disproportionate scatter at stress levels, which accounts for the complexity in the re-analysis. Moreover, fatigue data can either be censored (runouts excluded) or uncensored,

whilst the statistical distribution of fatigue life at a given stress level is assumed to be lognormal depending on the approach. Non-cutting-edge approaches are also known to be applied in the industry. For instance, the design by eye approach [13] is a very basic approach which is applied by drawing a line that follows the experimental data yet providing a “little white space” between these points and the design curve. Clearly, this design curve does not depend on a distribution, is subjective and lacks consistency across the board.

Considering the linear schematisation of the S–N curve in the MCF (see Fig. 1); one of the linear functions that is commonly used in a log-log representation is [14,15]:

$$\log N_f = C_0 + C_1 \log \sigma \quad (1)$$

where N_f is the fatigue life and σ is the stress level. C_0 and C_1 are the intercept and inverse slope constants respectively which are dependent on the fatigue data. The inverse slope determines the sensitivity of the material to fatigue, and a lower value indicates that the material is more sensitive to small changes in stress or strain amplitude. At any point on the curve, equation (1) is similar to Basquin’s equation. Basquin’s equation assumes a power-law relationship between the stress level and the number of cycles to failure [16,17]. Consider, for example, two reference points in the HCF regime, one defined as (σ_0, N_A) at the endurance limit and any other point, the corresponding equation (often referred to as Wöhler’s equation) can then be written as:

$$\sigma^k N_f = \sigma_0^k N_A = \text{constant} \quad (2)$$

where k is the negative inverse slope ($k = -C_1$) as defined in Fig. 1.

In the challenging scenario briefly summarised above, the aim of this paper is to review some of the standardised methods used for practical design in the MCF regime. These methods have been established over the decades using statistical approaches. The outputs from these approaches are analysed based on the assumption that the curve is linear. Virtual sample sets with varied statistical properties and fatigue data sets from the literature will be used for analysis. This quantitative review will exclusively concentrate on failures in the range of $10^3 \div 10^7$ cycles to failure, a range commonly used in the industry for design purposes. Exploring the methodologies employed in the HCF and beyond will constitute a key aspect of the upcoming work in this field, and it will be addressed accordingly. This will encompass approaches to materials that lack a fatigue limit, and analyses of the S–N curve around knee points. The next section explains the characterisation of the S–N curve in the MCF regime and its application in fatigue design.

2. S–N Curve and associated scatter band: theoretical schematisation

An essential consideration is the definition of the failure criterion used to generate data for S–N curves. Fatigue life typically comprises three phases: initiation, propagation, and final breakage. While theoretically, any of these phases could establish a suitable failure criterion, the choice influences the appearance of points on the S–N curves, leading to distinct fatigue curves. This is the reason why, normally, S–N curves are generated experimentally by adopting crack initiation as the failure criterion. In this setting, crack initiation is usually defined as the number of cycles required to initiate a technical crack with a length of the order of a few millimetres. An alternative solution is to define the crack initiation lifetime which results in a given reduction of the specimen stiffness. The criterion being adopted is always established prior to the investigation and generation of fatigue datasets. Further to this clarification, this paper maintains focus on the statistical analysis of data sets generated by using the initiation phase as the failure criterion.

The mean S–N curve plotted from the experimental data has a probability of survival $P_s = 50\%$, from which the fatigue limit (if it exists) or the endurance limit σ_0 is calculated. The fatigue limit is the theoretical stress level which a component survives without failure. Meanwhile, the endurance limit is the reference stress extrapolated in the HCF regime at N_A cycles to failure. The specific number of cycles chosen as the reference point may vary depending on factors such as material properties, application, and engineering standards or regulations, all of which are essential for design and analyses purposes. In this paper, the endurance limit is used and estimated at $N_A = 2 \times 10^6$ cycles for analyses purposes.

Fatigue tests which are terminated after surviving a specified maximum number of cycles (referred to as runouts) are treated differently by different analysis methods. In some methods, runouts are considered failures [15], whereas in others, they are entirely disregarded (censored) [17–19]. However, both approaches tend to underestimate the variation around the fitted line, as indicated by the standard deviation. In this paper (detailed in section 4), censored data sets are used to estimate the mean curve [5,14] and the endurance limit.

How is the design curve derived for the mean S–N curve? The design curve and corresponding design stress are determined by considering the variability in the fatigue data points. Through statistical analysis, the design stress ($\sigma_{0,P\%}$) based on the design curve at a given probability of survival P is obtained by shifting the mean curve by a scatter factor K_D as illustrated in Fig. 2. Therefore, the design stress/curve depends on the

size of the scatter factor, which in turn is dependent on the approach and the recommended probability of survival. This is the key focus of this paper (See section 4). For example, Eurocode 3 (EN1993-1-9) suggests a probability of survival of at least 97.7% to design welded joints against fatigue [5,15,20].

A confidence interval represents the range of stress levels for which the estimated endurance limit is likely to lie, based on the sample data. The confidence interval depends on the chosen confidence level, which indicates the probability that the estimated range will contain the true endurance limit. Suppose the endurance limit is calculated for a probability of survival $P\%$ (i.e. $\sigma_{0,P\%}$), the maximum value of this endurance limit at this probability is the value estimated at $1-P\%$. (i.e. $\sigma_{0,(1-P)\%}$). The interval between these stress levels is known as the confidence interval, and its size is referred to as the scatter band, τ_σ . This scatter band is extrapolated for the mean curve and serves as a visualisation tool to indicate the accuracy of estimation from experimental data sets. It makes use of statistical analysis to represent the uncertainty in the estimate of the S–N curve and is calculated as the ratio between the reference stress in the HCF regime for $(1-P)\%$ and $P\%$ probabilities of survival (see Fig. 2). The size of the scatter band is, therefore, dependent on the chosen approach as well.

Returning to the previously summarised challenges, the first of which was the generation of the S–N curve from a set experimental result, and the second challenge the determination of the associated scatter band with a probability of survival, what follows is a description of how these challenges can be addressed using some standardised approaches. The S–N curve problem is then addressed using the approach suggested by ASTM and its confidence interval [5]. The scatter bands problem is addressed using approaches suggested by the IIW, the ASTM and the LRM. In the considered fatigue lifetime region, it is assumed that the distribution of the logarithm of the fatigue life is normal at each stress level. However, this is not always the case, since different materials show different behaviours in the medium-cycle fatigue regime. Accordingly, the validity of this initial hypothesis must be checked before determining the associated scatter band. This is discussed below.

3. The mean S–N curve determined according to the ASTM

To determine a mean S–N curve from a set of experimental data, there are some essential assumptions that need to be considered [5,13,18,20–26]. In addition to these assumptions, Refs. [26,27] further emphasise the requirement to test several identical specimens at different stress levels such that the stress-life approach can be accurately utilized. Ref. [5] further emphasises the necessity of replication and suggests that the design curve with a probability greater than 50% is only as good as its level of replication. The suggested replication levels from Refs. [15,20,28] are summarised in Table 1. What follows is a description of these assumptions which are common to all methods.

3.1. Assumptions to determine mean S–N curves

For the statistical methods mentioned above to be consistent and accurate for S–N curves in the MCF region, the following arguments are required to be true. These arguments are essential in designing the S–N field around the mean curve.

Table 1
Minimum number of specimens and replication requirements for testing [11].

Type of test	Minimum Number of specimens	Replication percentage (%)
Preliminary and exploratory	6–12	17–33
Research and Development testing of components	6–12	33–50
Design data	12–24	50–75
Reliability data	12–24	75–88

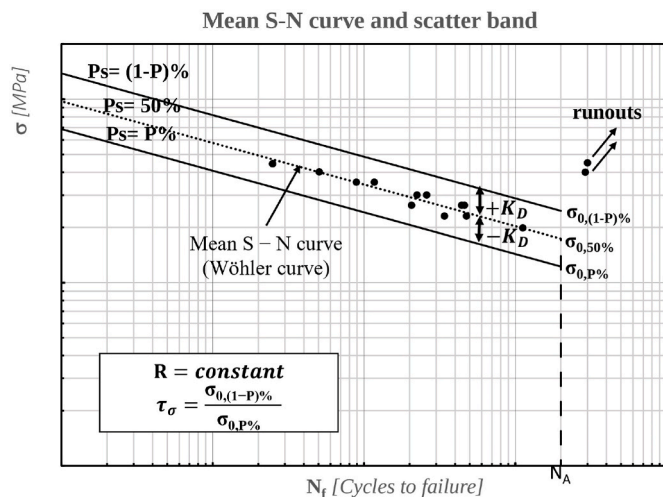


Fig. 2. The mean S–N curve showing the nature of the scatter factor K_D , the reference stress levels $\sigma_{0,P\%}$ at a probability of survival P , and the definition of the scatter band.

3.1.1. Linearity

The relationship linking fatigue life and the stress level in a log-log representation must be linear [5,15,28], assuming that the stress range chosen during testing corresponds to the linear section of the S–N curve in the MCF regime. There are a few possible linear relations used in fatigue [26] and the most common linear relationship in the log-log schematisation is defined in equation (1). This equation is valid only within set limits of the lifecycle of a specimen, for which the lower limit corresponds to the endurance/fatigue limit and the upper limit the transition region into LCF regime which varies depending on the material, into the static strength of the material specimen. Each stress level produces a unique impact on the fatigue life, and if this is not the case, then the assumption of linearity is invalid, and the Analysis of Variance (ANOVA) statistical model calculations are executed. In this case, the variance procedure uses F-tests to compare variances amongst duplicates in the data with the variance of the estimated population. If the variance within the replicates is far less than the variance in the estimated line, then linearity assumption is rejected.

3.1.1.1. Checking the condition of linearity. To verify the condition of linearity, the test statistic is employed in the null hypothesis. This involves using the F-distribution, which is effective in comparing the variances of two or more sample sets derived from continuous data sets with continuous distributions [5,15]. The critical values of the F-distribution are determined based on the desired level of confidence, which can be obtained from the F-tables in Refs. [26,29,30]. The degrees of freedom, denoted as n_1 and n_2 are derived from the two respective sample sets.

To determine if a fatigue dataset is linear, the sample data set can be grouped into two subsets. The first subset consists of the stress levels used to generate the data and the second subset considers all individual specimens independently. Suppose there are l number of stress levels with m replicates in the first subset with weighted averages $\overline{\log N_{fi}}$ representing the average life at each stress levels. ($i = 1..l, j = 1..m$). This weighted fatigue life has a degree of freedom defined as $n_1 = l - 2$. The second subset of the data is treated as the complete set of experimental data without any replications, has degrees of freedom $n_2 = n - l$, where n is the overall sample set. To determine the critical value F_p , the two entries n_1 and n_2 are used as:

$$F_{p\text{cal}} = \frac{n_1}{n_2} = \frac{l-2}{n-l} \quad (3)$$

Similarly, the F_p calculated is compared to the $F_{p\text{crit}}$ value calculated using the equation:

$$F_{p\text{crit}} = \frac{\sum_{i=1}^l \frac{m_i (\log(N_{fi}) - \overline{\log N_{fi}})^2}{(l-2)}}{\sum_{i=1}^n \sum_{j=1}^{m_i} \frac{(\log(N_{fji}) - \overline{\log N_{fji}})^2}{n-l}} \quad (4)$$

in which $\log N_{fij}$ ($i = 1..l$ and $j = 1..m$) is the logarithm of life at the replication level. The stress levels are carefully chosen to fall within the medium cycle fatigue region [5,22]. The null hypothesis is then used to determine linearity of the data set as follows:

Null Hypothesis.

- $F_{p\text{cal}} \leq F_{p\text{crit}}$; Null hypothesis confirmed, linearity model consideration can be adopted
- $F_{p\text{cal}} > F_{p\text{crit}}$; Null hypothesis is rejected and a Non-linear model of some form: $\log N_f = C_0 + C_1 \log \sigma_i + C_2 \log \sigma_i^2$, where C_0 , C_1 and C_2 are polynomial constants that describes the envelope of the curve.

Where the null hypothesis cannot be confirmed, Ref. [5,15] suggests that the non-linear consideration is adopted. Under this approach, the estimated mean curve is approximated as:

$$\log N_f = C_0 + C_1 \log(\sigma_i - C_2) \quad (5)$$

In this case, C_0 and C_1 are as defined previously while C_2 is a fatigue limit term. Other examples of non-linear considerations are defined by Refs. [14,15,31]:

$$\log N_f = C_0 (\log \sigma_i)^{n_1} + C_1 (\log \sigma_i)^{n_2} \quad (6)$$

Generally, a simple non-linear approach is defined as:

$$\log N_f = C_0 + C_1 (\log \sigma_i) + C_2 (\log \sigma_i)^2 \quad (7)$$

where C_0 , C_1 and C_2 are empirical constants that define the fatigue life [12,32]. Non-linear schematisations are not the focus of this paper. However, it is worth acknowledging the effects that the constants in equation (7) have on the shape of a fatigue curve. Specifically, C_0 defines a position on the ordinate axis, resulting in a parabola that either opens upwards or opens downwards. The shape of the parabola is determined by the sign of C_2 . A positive C_2 causes the parabola to open upwards, with C_0 determining the minimum point on the estimated curve. Conversely, a negative C_2 , positions C_0 as the maximum point on the estimated mean curve. For very small values of $\log \sigma_i$, the second term does not significantly impact on the shape of the curve. However, C_1 translates the turning point of the parabolic mean curve depending on its magnitude and direction. The translation is diagonal while ensuring that curve includes the point C_0 . A positive C_1 translates the turning point onto the third quadrant, while a negative C_1 will translate the turning point onto the fourth quadrant.

It is also important to acknowledge the significance of the bilinear and hyperbolic models proposed in Refs. [7,8] for ultra-high-cycle regimes, particularly when dealing with large data sets. These models provide valuable insights and are based on non-linear considerations. However, a comprehensive discussion of these non-linear aspects is beyond the scope of this paper.

3.1.2. Essential statistical assumptions in addition to linearity

Log normal distribution: fatigue life is normally distributed or log-normally distributed in the log-log space for any stress levels σ_i . This is achieved by assessing whether the probability plot in the log-log space departs from the mean S–N curve follows a linear trend. In this paper, it is assumed that, at each stress level, the fatigue life has a normal distribution around the mean life.

Statistical Independence: fatigue life of any single sample is considered independent of the fatigue lives of other samples or data points. This independence can be verified by examining the residuals of $\log N_f$ in the datasets to ensure there are no recurrent patterns. If any noticeable patterns emerge the data is grouped accordingly and an analysis of variance (ANOVA) is conducted on the data.

Homogeneity and standard deviation: it is assumed that, at each stress level, the variance and standard deviation of fatigue life are constant. This assumption is verified by examining the plots of residuals from the mean curve with $\log \sigma$. To assess statistical homogeneity, Bartlett's test is applied if the fatigue life is normally distributed at each stress level; otherwise, Levene's test is used [12,20,26]. It is important to note that while these tests were relevant, they are not the primary focus of this paper and are not included in this review.

3.2. Fitting the S–N mean curve and confidence interval

Having asserted the above essential assumptions, the first aspect considered in this paper is to determine which approach among the various linear models will be used to fit a mean S–N curve onto an experimental fatigue data set. The linear regression method is employed, and the statistical approaches selected for this study uses the same method for the mean curve. This regression analysis uses the least squares approximation [14,16,32] to determine the parameters of the mean curve by minimizing the sum of the squares of the differences

between the observed dependent variable (fatigue life) and the output of the linear function of the independent variable (stress levels). Consequently, estimates of the slope and intercept are generated. This is possible by applying a log – log plot of the data with the assumption of a log-normal distribution of fatigue life at each stress level. The estimated mean curve has a 50% probability of survival, (i.e. $P_s = 50\%$) and the function that defines the equation of the regression curve defined in equation (1) has an error band defined as [1,32]:

$$\log N_f = C_0 + C_1 \log \sigma_i + \xi \tag{8}$$

where ξ is the unknown random measurement error connected with the estimation of fatigue life. The maximum likelihood method can also be used to determine the parameters C_0 and C_1 because of its good statistical properties [33,34]. However, the main disadvantage is that the likelihood equations need to be derived for each specific distribution, which can be cumbersome. To simplify this process, the least squares approach is used to estimate the parameters in the mean curve [14,15, 35]. Thus C_0 and C_1 are estimated at the mean points of the dataset as:

$$C_1 = \frac{\sum_{i=1}^n [\log(\sigma_i) - \overline{\log \sigma_i}] [\log(N_i) - \overline{\log N_i}]}{\sum_{i=1}^n [\log(\sigma_i) - \overline{\log \sigma_i}]^2} \tag{9}$$

$$C_0 = \overline{\log N_i} - C_1 \overline{\log \sigma_i} \tag{10}$$

in which n is the sample set and $i = 1, 2, \dots, n$. $\overline{\log \sigma_i}$ is the mean of log stress levels and $\overline{\log N_i}$ is the mean of the log of fatigue life. By taking the natural logs in equation (2) and comparing with equation (8), the inverse slope k , whose value is of great significance in fatigue analysis and design, and in the least squares estimation is defined as:

$$k = - C_1 \tag{11}$$

By substituting the inverse slope in equation (8) and assuming negligible error in estimating the parameters of the mean curve, the equation for the mean S–N curve can be written as:

$$\log N_f = C_0 - k \log \sigma_i \tag{12}$$

According to this schematisation the endurance limit $\sigma_{0.50\%}$, at the corresponding reference number of cycles N_A , can be determined as,

$$\sigma_{0.50\%} = \left[\frac{10^{C_0}}{N_A} \right]^{\frac{1}{k}} \tag{13}$$

Having estimated the parameters in the mean S–N curve, what follows is an estimate of the amount of uncertainty associated with the mean curve otherwise known as the confidence interval.

3.2.1. Confidence level of the estimators C_0 and C_1 and the mean S–N curve

The parameters defining the mean S–N curve C_0 and C_1 are estimates and have associated confidence intervals. This confidence level defines the probability that each parameter will fall within a specified range of values. With a 95% confidence level, it is expected that 95% of the time the suggested parameter will exist within this limit.

Assuming that all the arguments described in section 3.1 are true, and the estimators of C_0 and C_1 are normally distributed irrespective of the sample size, a t-distribution is used to determine the confidence interval for these parameters [5,15,22]. The confidence interval for C_0 is defined as [5,15]:

$$C_0 - t_p s \sqrt{\frac{1}{n} + \frac{\overline{\log \sigma_i}^2}{\sum_{i=1}^n (\log \sigma_i - \overline{\log \sigma_i})^2}} \leq C_0 \leq C_0 + t_p s \sqrt{\frac{1}{n} + \frac{\overline{\log \sigma_i}^2}{\sum_{i=1}^n (\log \sigma_i - \overline{\log \sigma_i})^2}} \tag{14}$$

where t_p is the critical value of the t-distribution patterning to a probability of survival P_s and s is the unbiased estimator of the standard deviation of fatigue life defined by equation (15) [20,26,29,30] where $\log N_i$ is the log of observed live at the stress level.

$$s^2 = \frac{\sum_{i=1}^n (\log N_{fi} - \log N_f)^2}{n - 2} \tag{15}$$

Similarly, C_1 will lie within the limits defined by,

$$C_1 - \frac{t_p s}{\sum_{i=1}^n \sqrt{\log \sigma_i - \overline{\log \sigma_i}}} \leq C_1 \leq C_1 + \frac{t_p s}{\sum_{i=1}^n \sqrt{\log \sigma_i - \overline{\log \sigma_i}}} \tag{16}$$

These estimations remain valid under the condition that the life estimation of a random sample is independent and all the previously defined assumptions hold true, with the additional requirement that there are no runouts in the fatigue data set.

3.2.2. Confidence level of the mean S–N curve

Based on the assumptions defined in section 3.1, the confidence interval for the mean curve is defined by

$$\log N_f = C_0 + C_1 \log \sigma_i \pm \sqrt{2F_p s} \sqrt{\frac{1}{n} + \frac{(\log \sigma_i - \overline{\log \sigma_i})^2}{\sum_{i=1}^n (\log \sigma_i - \overline{\log \sigma_i})^2}} \tag{17}$$

The confidence interval uses a constant F_p , known as the critical value of the F – distribution (otherwise called the Snedecor distribution), which is read from statistical tables as in Refs. [5,14,15,27]. In addition, the actual mean S–N curve is only an approximation of the best straight line representing the dataset in the interval of the stress levels used during testing [5], with estimators defined with a confidence level of 95%. Consequently, confidence levels for the entire mean S–N curve with a confidence greater than 95% are not recommended for this mean curve and this method is not recommended to extrapolate the S–N curve beyond the test interval.

The curves generated using equation (17) are hyperbolas which are closest to the mean curve at the mean points as illustrated in Fig. 3.

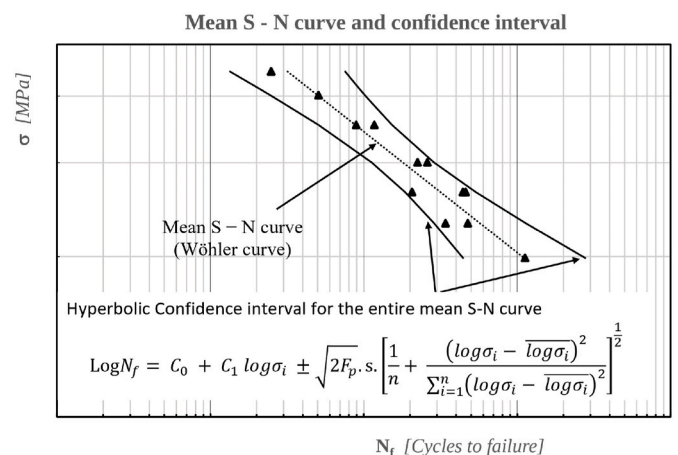


Fig. 3. Hyperbolic curves showing the confidence interval of the mean curve and the associated data points.

These hyperbolic curves are of little interest to design engineers and will be transformed to parallel lines that provide the confidence interval along any stress level [5,12,32] and are used to generate the scatter band. The length of the perpendicular bisector at the mean point to the mean S–N curve determines the position of the parallel curves and this is half the size of the confidence interval. The endurance limit $\sigma_{0,P\%}$ at N_A cycles to failure of the mean curve characterised by a probability of survival $P_s = P\%$ is estimated as:

$$\sigma_{0,P\%} = \left[\frac{10^{(C_0 - K_{D(ASTM)s})}}{N_A} \right]^{1/k} \quad (18)$$

$K_{D(ASTM)}$ is the scatter factor and is defined as:

$$K_{D(ASTM)} = \sqrt{\frac{2F_p}{n}} \quad (19)$$

The critical value F_p , of the F – distribution is dependent on the probability of survival. In a similar way, the endurance limit $\sigma_{0,(1-P)\%}$, at N_A cycles to failure of the line delimiting the calculated scatter band, with a probability of survival $P_s = (1 - P)\%$ is defined as:

$$\sigma_{0,(1-P)\%} = \left[\frac{10^{(C_0 + K_{D(ASTM)s})}}{N_A} \right]^{1/k} \quad (20)$$

These parallel lines, equidistant from the mean S–N curve define the region for the confidence interval of the mean S–N curve.

Before proceeding to address the second challenge of generating fatigue design curves and their associated scatter bands, it is necessary to examine the wide range of available approaches that are applicable in the industry.

3.3. Other methods of constructing fatigue design curves

To begin with, assume that the approaches considered here would generate the mean curve based on the assumptions defined in section 3.1 and also use the linear considerations and method described in section 3.2 irrespective of the linear model applied [15].

State of the art methods across the industry generally approach the fatigue design problem by using scatter factors which are dependent on their statistical considerations and in-service application of the component. According to Ref. [14], most engineering approaches prefer the 2-sigma or 3-sigma design curves in which the mean S–N curve is shifted two to three standard deviations to generate the design curve. However, this approach fails to attest for the statistical distribution of fatigue life. The general equation to construct the design [14,24] curve is defined by:

$$\text{Log } N_{f,D} = \text{Log } N_f - K_D s \quad (21)$$

where $\text{Log } N_{f,D}$ is the natural logarithm of the estimated design life, K_D is a scatter function that is dependent on the probability of survival and sample size n , and s is the standard error of the estimated life N_f [14,27]. The different approaches all use different considerations to determine the scatter factor, which is dependent on the industry and application.

3.3.1. Lower 2-sigma or 3-sigma design curves

This design curve is determined by subtracting 2 or 3 times the standard deviation from the fitted mean curve. Following from equation (21), $K_D = 2$ or $K_D = 3$ [14]. Similarly, Ref. [13] suggests that the scatter factor K_D is to be determined by choosing a suitable probability of survival. However, this method does not address the confidence level problem associated with the parameters of the mean S–N curve. Because of this limitation therefore, this method will not be considered beyond this point.

3.3.2. One dimensional tolerance limit

For a one-sided tolerance limit of a normal distribution where only one variable is involved, K_D will depend on the probability of survival P

and the confidence level γ [1,13] and is defined by:

$$K_{D(\text{one-sided-T})} = k_{\gamma,(n-2)} \sqrt{1 + \frac{1}{n}} \quad (22)$$

where $k_{\gamma,(n-2)}$ is the tolerance limit factor for a confidence level γ and $n - 2$ degrees of freedom. $K_{D(\text{one-sided-T})}$ represents the scatter factor generated using the one-sided tolerance limit approach [15].

This method is applicable when all samples are replicated at each stress level [15] with the fatigue life having a normal distribution. More so, the one-sided tolerance limit is valid if the assumptions in generating the mean curve are tested and verified. As much as this approach is efficient for very complex cases, the assumption of log-normal distribution and uniformity of variance must be verified and confirmed before application. In case the distribution is not log-normally distributed [13, 15], a different approach is recommended [27]. Because the log-normal distribution assumption is not considered by this approach, this reduces the scope for which it is applicable. More so, when applied to a two dimensional case, this method fails to accurately estimate the uncertainty in the two parameters involved [13]. This method is also quite difficult to implement and its conservativeness may not be very useful for all applications. Tolerance limits are more sensitive to slight deviations from the assumed normality compared to prediction limits [15,26]. In addition, the use of tolerance limits does not necessarily correspond with earlier practice and hence may not be compatible with present design rules. This therefore suggests that it is not always suitable to base the design curve on tolerance limits. Despite the above, tolerance limits still constitute an essential tool in studying the responsiveness of a design curve in relation to the population. Hence, tolerance limits should be used to justify our design curves only for small sample populations. Because of these limitations, this approach will not be considered for analysis in this paper.

3.3.3. Owen Lower Tolerance Limit

This approach guarantees a confidence limit γ at any given stress or strain level and the scatter factor $K_{D(\text{OWEN})} = K(x; V)$ in which the function $V(p, \gamma, n, m, x)$ is such that p is the probability of survival, γ is the confidence limit, n is the dimension of the stress level vector and m is the number of undetermined parameters in the mean curve [13,14,36]. $K_{D(\text{OWEN})}$ values are read from tables in Refs. [14,37]. They depend on the sample sizes, reliability levels, and confidence levels. According to this approach, the design curve is:

$$\text{Log } N_{f,D} = \text{Log } N_f - K_{D(\text{OWEN})} s \quad (23)$$

The Owen lower tolerance limit method assures the same confidence level at any stress level and predicts intervals that agree with other approaches. However, this is very applicable in non-linear approaches, and is also dependent on the distribution at each stress level and the total specimen number [13]. Because this review paper assumes a homogeneity of standard deviation, this approach will not be included in the review process considered in this paper.

3.3.4. The simultaneous Tolerance Limit

According to the simultaneous tolerance limit approach, the scatter factor $K_{D(\text{Sim})}$ is as defined in equation (25) and $\chi_{n-2}^{2,\alpha/2}$ is the $\alpha/2$ quantile of the χ_{n-2}^2 distribution.

$$K_{D(\text{Sim})} = \sqrt{2F_p} \sqrt{\frac{1}{n} + \frac{(\log(\sigma_{a,i}) - \overline{\log \sigma_{a,i}})^2}{\sum_{i=1}^n (\log(\sigma_{a,i}) - \overline{\log \sigma_{a,i}})^2}} + N(P) \sqrt{\left(\frac{n-2}{\chi_{n-2}^{2,\alpha/2}} \right)} \quad (24)$$

The simultaneous tolerance limit guarantees that 100 γ percent of the time, the probability of failure is always less than $1 - P$ for all stress levels at the same time [13]. Similar to the Owen Lower Tolerance Limit, this approach will not be reviewed in this paper because it is good for

very complex data distributions at different stress levels and its complexity in application compared to very simple linear models.

3.3.5. Parallel Tolerance Interval (PTI) for P-S-N surface, Bowden and Graybill approach

The scatter factor $K_{D(PTI)}$ under the parallel tolerance approach is defined in as:

$$K_{D(PTI)} = C^* + z_p \sqrt{\left[\frac{1}{n} + \frac{(n-2)}{\chi^2_{(n-2), (1-\gamma_2)}} \right]} \quad (25)$$

The parameter C^* is dependent on the variance between the maximum and the minimum stress level, the probability of survival and the Bowden and Graybill's factor which depends on the probability of survival and is read from statistical tables as in Ref. [32]. z_p is the standard normal deviate such that the probability of survival is always enclosed within $\pm z_p$. More so, $(1 - \gamma_2)$ becomes the upper confidence limit of the standard deviation that needs the γ_2 point of the chi-square distribution with $(n - 2)$ degrees of freedom. This method depends on the statistical Bowden and Graybill's factors and these factors and their application has not been observed anywhere else in the literature. Thus, the approach will not be considered beyond this section.

3.3.6. TWI approach

The TWI uses an approach that employs the mean curve from the experimental data to compare with a predetermined target curve [28], which depends on the material and application. In this case, the target curve has predefined curve parameters and is always a factor above the standard design curve. For fatigue data with an inverse slope similar to the target curves, the design curve is constructed by simply comparing the intercepts. The intercept of the test design curve C_{0D} is defined in equation (25) where C_0 is the intercept of the mean standard curve in which SMF is the stress modification factor of the test data relative to the standard S-N curve patterning to the required level of confidence. This approach is limited to data with inverse slopes similar to those of standard curves, hence was not reviewed in this paper.

$$C_{0D} = C_0 - 2s - C_1 \text{LogSMF} \quad (26)$$

3.3.7. The ASME Boiler and Pressure Vessel code

According to this model the design curve for the fatigue mean curve is generated by using a scatter factor of 20 in the direction of the stresses [13]. Although this produces results that are very conservative, this approach takes into account some of the parameters that influence fatigue behaviour, such as the size, the environment, the surface finish, and the scatter of data [24,36]. This is particularly accurate for very high pressure service environments for low cycle fatigue. This approach is very useful for critical design and peculiar to pass pressure applications. Because of this reduced scope of application, this approach will not be considered in this review paper.

4. The design curves (scatter factors) according to the ASTM, IIW and Linear regression method

Having determined the mean curve that is common to all the approaches and also explored some of the approaches that are used in the industry, this section will explain how the standardised methods suggested by the ASTM, the IIW and the Linear Regression Method are used to construct the design curve based on a probability of survival, and the associated scatter bands using their respective scatter factors. In particular, the ASTM method uses prediction limits to determine a design curve and scatter band.

4.1. ASTM scatter factor approach of prediction limit approach

According to Ref. [5], the ASTM method assumes the considerations

described in section 3.1 for censored data. In this standard, the S-N relationships are approximated by $\log - \log$ plots in the MCF regime where it is linear. ASTM standard reiterates the variance be defined as:

$$s^2 = \frac{\sum_{i=1}^n (\text{Log } N_f - \text{Log } N_i)^2}{n - 2} \quad (27)$$

wherein the term $(n - 2)$ in the denominator is the adjusted degrees of freedom patterning to C_0 and C_1 and enables the variance to be unbiased. In cases where the data is fitted to standard curves with predetermined parameters, for instances in approaches where $C_1 = 3, 5, \dots$, the degrees of freedom in this case is adjusted to $n - 1$. The prediction limits for which the lower limit is the design curve is defined as [5,15,22,29]:

$$\text{Log } N_{f,D} = C_0 + C_1 \log \sigma_i \pm \sqrt{2F_p} s \sqrt{1 + \frac{1}{n} + \frac{(\log \sigma_i - \overline{\log \sigma_i})^2}{\sum_{i=1}^n (\log \sigma_i - \overline{\log \sigma_i})^2}} \quad (28)$$

$$K_{D(ASTM)} = \sqrt{2F_p \left(1 + \frac{1}{n}\right)} \quad (29)$$

Following on from equations (28) and (29) the reference stress at the reference cycle is as defined in equation (13). The prediction limit at this point, based on a probability of survival, is established. Subsequently, the endurance limit $\sigma_{0,P\%}$, with a probability of survival $P\%$, is determined using the equation [5,15,24]:

$$\sigma_{0,P\%(ASTM)} = \left[\frac{10^{(C_0 - K_{D(ASTM)s})}}{N_A} \right]^{\frac{1}{k}} \quad (30)$$

Similarly, the endurance limit in error at $(1 - P)$ delimiting the interval generated by the design curve can be calculated using the equation:

$$\sigma_{0,(1-P)\%(ASTM)} = \left[\frac{10^{(C_0 + K_{D(ASTM)s})}}{N_A} \right]^{\frac{1}{k}} \quad (31)$$

The scatter band τ_σ , according to the ASTM is calculated as:

$$\tau_{\sigma(ASTM)} = \frac{\sigma_{0,(1-P)\%(ASTM)}}{\sigma_{0,P\%(ASTM)}} \quad (32)$$

4.2. IIW scatter factor approach and scatter band

The IIW also takes into consideration the assumptions explained in section 3.1. The mean curve is generated using the same procedure as defined using estimates detailed in section 3.2 [26]. Accordingly, the scatter factor used to calculate the scatter band with a 95% confidence level uses a student t-distribution and is defined as:

$$\text{Log } N_{f,D} = C_0 + C_1 \log \sigma_i \pm t s \sqrt{1 + \frac{1}{n} + \frac{(\log \sigma_i - \overline{\log \sigma_i})^2}{\sum_{i=1}^n (\log \sigma_i - \overline{\log \sigma_i})^2}} \quad (33)$$

C_0 and C_1 are constants as described in section 3.2. t is the corresponding percentage point of the student's t-distribution with of degrees of freedom equal to $n - 2$ and s^2 is the best guess of the variance around the mean curve as defined in equation (27).

For a large sample sizes, the IIW method approximates the term $1/n$ in equation (33) to zero, in accordance with Gurney and Maddox as reported in Ref. [26]. Consequently, this term in the prediction equation is ignored for a sample size of 20 or more, which only accounts for a 2% error in the estimation of the width of the scatter band [20,26]. For a sample set less than 10, the term under the square root sign assumes the value of one, and the degrees of freedom is adjusted to $f = n - 1$ as summarised in a Table 2. For $n \leq 10$, consider the extreme case under

Table 2
Table of values of F_p according to STP 313 (4) as quoted in [11].

Degrees of freedom, n_2	Degrees of freedom n_1			
	1	2	3	4
1	161.45	199.50	215.71	224.58
	4052.2	4999.5	5403.3	5624.6
2	18.513	19.000	19.164	19.247
	8.503	99.000	99.166	99.249
3	10.128	9.5521	9.2766	9.1172
	34.116	30.817	29.457	28.710
4	7.7086	6.9443	6.5914	6.3883
	21.198	18.000	16.694	15.977
5	6.6079	5.7861	5.1922	5.1922
	16.258	13.274	12.060	11.392
6	5.9874	5.1433	4.7571	4.5337
	13.745	10.925	9.7795	9.1483
7	5.5914	4.7374	4.3468	4.1203
	12.246	9.5466	8.4513	7.8467
8	5.3177	4.4590	4.0662	3.8378
	11.259	8.6491	7.5910	7.0060
9	5.1174	4.2565	3.8626	3.6331
	10.561	8.0215	6.9919	6.4221
10	4.9646	4.1028	3.7083	3.4780
	10.044	7.5594	6.5523	5.9943
11	4.8443	3.9823	3.5874	3.3567
	9.6460	7.2057	6.2167	5.6683
12	4.7472	3.8853	3.4903	3.2592
	9.3302	6.9266	5.9526	5.4119
13	4.6672	3.8056	3.4105	3.1791
	9.0738	6.7010	5.7394	5.2053
14	4.6001	3.7389	3.3439	3.1122
	8.8616	6.5149	5.5639	5.0354
15	4.5431	3.6823	3.2874	3.0556
	8.6831	6.3589	5.4170	4.8932

this condition where $n = 1$. This means that $\frac{1}{n} = 1$ and the point variance of each of the data is always less than one. Therefore, the term under the square root sign in equation (33) can be approximated to 1 without great loss in the size of the scatter band [26]. Similarly for $n \geq 20$, the extreme case corresponds to $n = \infty$, for which $1/n \approx 0$. The degrees of freedom is adjusted which reduces the size of the corresponding scatter band by a very negligible amount. The scatter factor $K_{D(IIW)}$, according to the IIW is calculated as:

$$K_{D(IIW)} = t \sqrt{1 + \frac{1}{n}} \quad (34)$$

Similarly to the other approaches under review, the endurance level $\sigma_{0,P\%(IIW)}$ for a probability of survival P is defined as in equation (35), while the endurance limit in error at the reference cycle $\sigma_{0,(1-P)\%(IIW)}$ is defined in equation (37).

$$\sigma_{0,P\%(IIW)} = \left[\frac{10^{(C_0 - K_{D(IIW)} s)}}{N_A} \right]^{\frac{1}{k}} \quad (35)$$

and

$$\sigma_{0,(1-P)\%(IIW)} = \left[\frac{10^{(C_0 + K_{D(IIW)} s)}}{N_A} \right]^{\frac{1}{k}} \quad (36)$$

Therefore, the scatter band generated according to the IIW is defined as,

$$\tau_{\sigma(IIW)} = \frac{\sigma_{0,(1-P)\%(IIW)}}{\sigma_{0,P\%(IIW)}} \quad (37)$$

4.3. The Linear Regression scatter factor approach and scatter band

According to the linear regression schematisation, the predicted mean curve follows the assumptions defined in section 3.1 [6,29,38]. The estimated constants C_0 and C_1 are also estimated using the method described in section 3.2. The endurance limit can be found by computing

σ_0 using equation (13). However, the variance is calculated as:

$$s^2 = \frac{\sum_{i=1}^n (\text{Log } N_f - \text{Log } N_i)^2}{n-1} \quad (38)$$

The unbiased condition is achieved by reducing the degrees of freedom by 1, i.e. $f = n - 1$ [1,38]. Subsequently the reference stress level at N_A cycles to failure for different probabilities can be computed using the standard deviation, reference stress level at P50% and another empirical constant, q , which is read from standard statistical tables for normal or log-normal distributions found in Refs. [5,29,37,38] and is dependent on the desired probability of survival, confidence level and sample set. In this case the endurance limit is defined as:

$$\sigma_{0,P\%(LM)} = \sigma_0 \left[\frac{N_A}{10^{\log(N_A) + qs}} \right]^{\frac{1}{k}} \quad (39)$$

This has been established by using the well-known Wöhler relationship which considers that for a material with a fatigue limit and a known value of the inverse slope k , this equation is always true. Alternatively, materials without a defined fatigue limit, the endurance limit is determined and equation (41) holds true whenever $N_f \leq N_{KP}$, where N_{KP} is the fatigue life at the knee point.

$$\sigma^k N_f = \sigma_0^k N_0 = \sigma_A^k N_A = \text{constant} \quad (40)$$

$$\sigma^{k_1} N_f = \sigma_{KP}^{k_1} N_{KP} \quad (41)$$

σ_i is the stress level corresponding to the fatigue life N_f at that point. Thus, the delimiting endurance limit is defined as:

$$\sigma_{0,(1-P)\%(LM)} = \sigma_0 \left[\frac{N_A}{10^{\log(N_A) - qs}} \right]^{\frac{1}{k}} \quad (42)$$

Similarly, the scatter band according to this approach can be written as:

$$\tau_{\sigma(LM)} = \frac{\sigma_{0,(1-P)\%(LM)}}{\sigma_{0,P\%(LM)}} \quad (43)$$

5. Application of the scatter factors and scatter bands

Setting out to explore the various approaches is achieved by applying them to both theoretical data sets and experimental fatigue data sets sourced from the literature. By analysing these diverse data sets uncovered patterns that will justify the application of each approach.

5.1. Application of the scatter factors and scatter bands on theoretical data

This section was intended to explore the impacts of the variation in fatigue data to the aforementioned approaches described in section 4. Particularly, the effects of varied statistical characteristics that define the scatter band. To achieve this, the authors have generated some theoretical data sets with defined parameters, by continuous correction and improvement until the desired statistical properties were achieved. The complexity in generating experimental data sets with desired statistical characteristics, and the cost and time involved have been the motivation in applying this approach. Moreover, it cannot be determined a priori if a set of specimens will generate data sets with pre-determined statistical characteristics. The inverse slopes chosen ranged from 30 to 3, which are common with plain and notched metals, and the spreads will vary from a base standard deviation to about three times the base standard deviations. The impact of percentage replication and degrees of freedom will also be investigated.

5.1.1. Variation of scatter band with change in slope

Consider fatigue data generated such that the inverse slope increases

as summarised in Table 4 such that each data set has the same level of spread in the direction of fatigue life. The replication level (see Table 1) of 75% is constant throughout which is a necessary requirement for experimental data to be used for design [12,27,32]. The mean curves produced by pairing each series column with the corresponding N_f (cycles) is shown in Fig. 4, as well as the design curves determined using the scatter factors described in the approaches previously.

The data for the various slopes have been randomly generated such that the resulting curve always lies within the same stress range and life range. Since these curves have not been systematically generated using reference points, the analysis will be limited only by how the scatter band changes with the various approaches.

According to the data summarised in Table 4, as the inverse slope increased, the size of the scatter bands for each approach reduces. Additionally, for very large values of inverse slope, it is observed that the size of the scatter bands converges to similar sizes. This convergence is illustrated in Fig. 5. Hence it is concluded that for fatigue data with equal variances in the direction of the fatigue life, the design curves described by the ASTM, IIW, and LRM approaches agree for high values of inverse slopes.

5.1.2. Change of scatter band with spread

The spread of statistical data shows how extreme values in a data set occur. The spread can be varied by either altering the range in the stress level, determining the variance, standard deviation, and/or determining the absolute deviations of the inter-quartile range. Table 5 shows data with increasing spread from one base standard deviation to three times the base standard deviations at each of the stress levels. This was the weighted spread with a replication level of 75%. Each graph is generated by considering the first column of Table 5, with each of the data series columns. The mean curves and the design curves are illustrated in Fig. 6.

The relationship between the weighted spread and the variance of the entire data set was not always straightforward. Increasing the weighted spread from one standard deviation to multiple standard deviations does not necessarily affect the overall variance. However, it has an impact on the endurance stresses of the design curves, causing them to decrease. This is reflected in the drop height of the design curves compared to the mean curve. It is noteworthy that the approach recommended by the ASTM is particularly influenced by an increase in the spread of fatigue data.

An increase in the design curve will generate a similar size in the error of probability of survival, in this case 95%. This is because the prediction limits are always symmetrical about the mean curve. Consequently, as the spread of fatigue data increases, the prediction limits also increase, as depicted in Fig. 7. The scatter bands expand with

Table 3

Calculating the size of scatter band which is dependent on sample size as recommended by the IIW.

Calculating estimate in error with small sample set	Calculating estimate in error with large sample set
$n \leq 10$ $\sqrt{1 + \frac{1}{n} + \frac{(X - X_m)^2}{\sum_{i=1}^n [X_i - X_m]^2}} = 1$ $Y(x) = \hat{Y}(X) - t * s$ $Y(x) = C_0 + C_1 * X_m \pm t * s.$ $s = \sqrt{\frac{\sum_{i=1}^n [Y_i - Y(x_i)]^2}{n - 2}}$	$n \geq 20$ $\frac{1}{n} = 0 \Rightarrow \sqrt{1 + \frac{(X - X_m)^2}{\sum_{i=1}^n [X_i - X_m]^2}}$ $Y(x) = \hat{Y}(X) - t * s *$ $\sqrt{1 + \frac{(X - X_m)^2}{\sum_{i=1}^n [X_i - X_m]^2}}$ $Y(x) = C_0 + C_1 * X_m \pm t * s.$ $s = \sqrt{\frac{\sum_{i=1}^n [Y_i - Y(x_i)]^2}{n - 1}}$

Table 4

Theoretical data such that the inverse slope increases. Each series in σ (MPa) is paired with column N_f (cycles).

σ (MPa)				N_f (Cycles)
Series 1	Series 2	Series 3	Series 4	
300	300	300	300	7301
300	300	300	300	1245
300	300	300	300	1685
300	300	300	300	4505
250	275	280	290	6498
250	275	280	290	12560
250	275	280	290	4510
250	275	280	290	6500
200	250	260	280	8250
200	250	260	280	16040
200	250	260	280	14456
200	250	260	280	11000
150	225	240	270	88001
150	225	240	270	94000
150	225	240	270	95254
150	225	240	270	89580
100	200	240	260	128100
100	200	240	260	121023
100	200	220	260	128600
100	200	240	260	127210

the increasing spread, and notably, the ASTM approach exhibits a more conservative stance compared to other approaches.

Within the same stress range, as the spread of the fatigue data increases in multiples of the variance, the endurance limit reduces and hence the design stress level also reduces. Thus, the scatter bands generated also increased as seen in Fig. 7. When considering a range of two standard deviations, the scatter bands produced by the ASTM, IIW, and LRM approaches exhibited similarity. However, as the spread of data increases beyond this range, the approaches start to diverge, showing differences of up to 50%. In such cases, the ASTM approach is more conservative in its predictions compared to the other approaches.

5.1.3. Impact of replication levels on approaches

Consider for example the data summarised in Table 6. The levels of replication and application is summarised in Table 1. The replication level is calculated as [5,28]:

$$Rep \% = 100 \left[1 - \frac{n_\sigma}{n} \right] \tag{44}$$

where n_σ is the number of stress levels and n is the total number of specimens. From this, the number of stress levels can be determined a priori based on the replication percentage, the number of specimens available and the approach used. The replication levels considered in these virtual data sets have been carefully selected such that the various replications levels summarised in Table 1 are analysed. The stress levels range has been kept constant as well as the overall spread of the fatigue life at $s \cong 0.18$. The only varied parameter in this case is the stress level and the number of specimens at the stress level. The various scatter bands generated using the approaches in this study have been summarised in Fig. 9. Clearly, the scatter bands remain constant as the percentage replication increases as illustrated by the graph in Fig. 8.

5.1.4. Impact of sample size on approaches

Table 1 details the various sample sizes in fatigue experiments in relation to the purpose for which the data is intended for. Accordingly, this sets a minimum sample set of six specimens with at least four stress levels such that there is always the presence of replicate data. Attention will be limited in this case to data for preliminary studies requiring just about 6–12 data points. Consider the data in Table 7 in which each set of data has the same sample standard deviation of about 0.9 and with at least one pair of replicate data in the sample sets. The stress level range is also constant and the only varying parameter is the degrees of freedom.

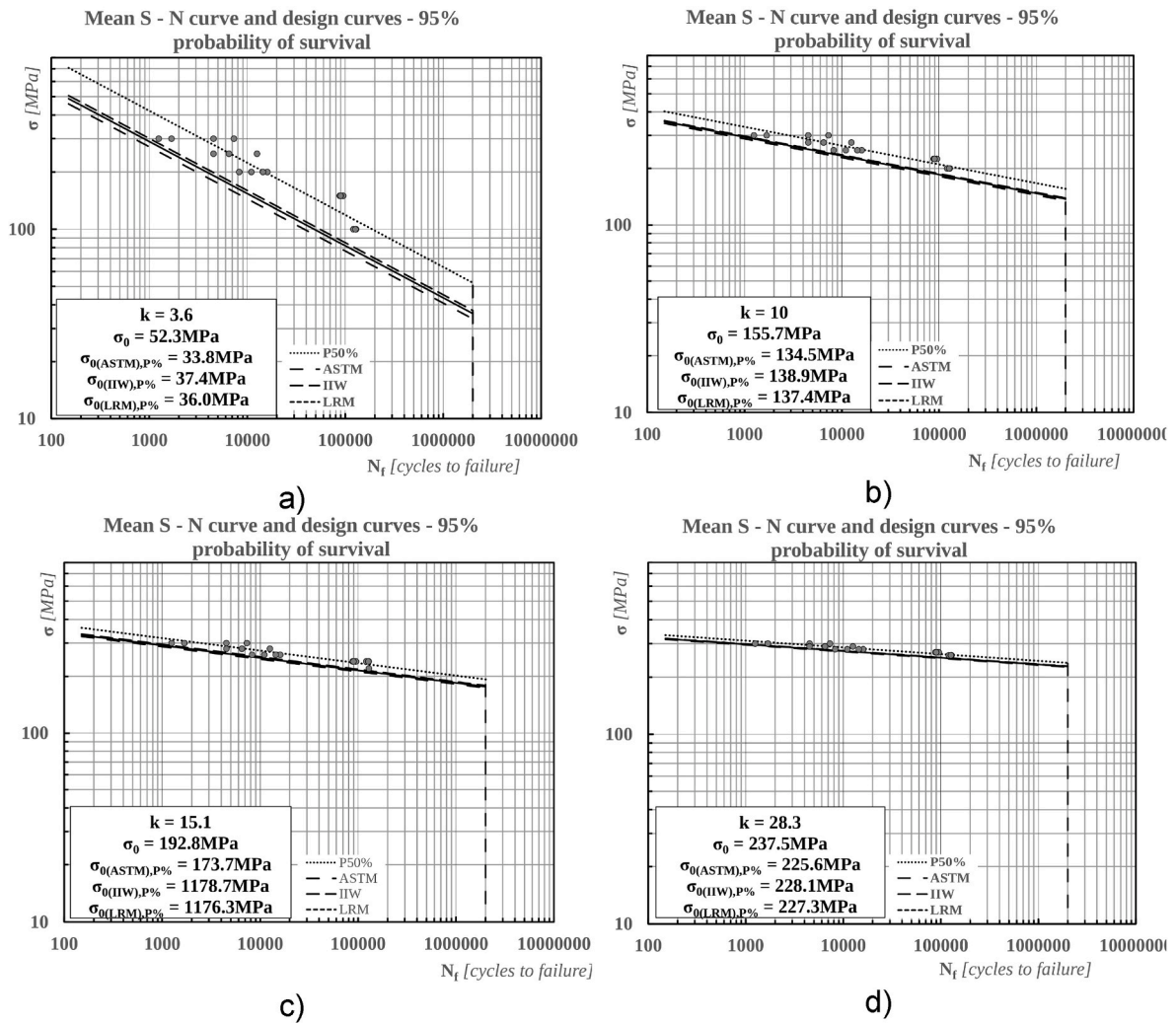


Fig. 4. Mean curves, design curves with the design stress levels for increasing inverse slopes values at a probability of survival of 95% for the data in Table 4 a) inverse slope 3.6, b) inverse slope 10, c) inverse slope 15.1 and d) inverse slope 28.3.

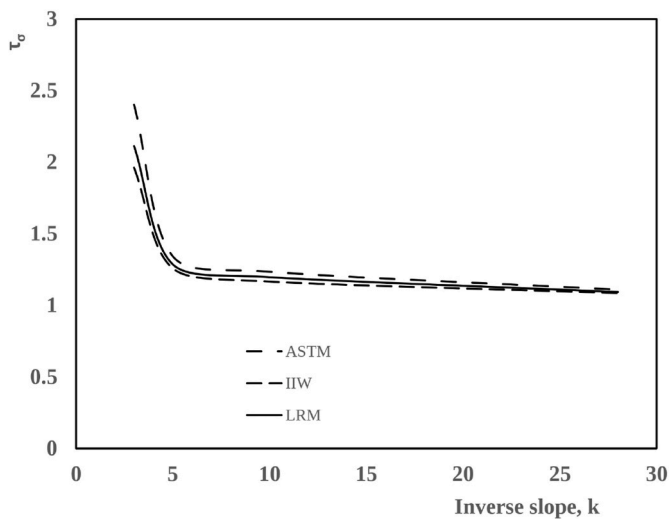


Fig. 5. The change in scatter bands with increasing inverse slope.

The graphs summarised in Fig. 10 illustrates how the scatter band changes as the degrees of freedom increases. It is evident that the size of the scatter band considering each of the approaches changes to the same

Table 5

Theoretical data generated such that the variance is increasing, while percentage replication, sample set and inverse slope kept fairly constant. The stress level is paired with each data column in N_f (cycles).

σ (MPa)	N_f (cycles)			
	Data 1	Data 2	Data 3	Data 4
300	3650	1650	1650	1020
300	3345	3345	3145	7145
300	3685	11295	19995	24869
300	10505	16505	20985	29985
250	5498	3599	5599	3599
250	11560	16750	22750	29120
250	3510	3510	2310	2310
250	5500	14500	20990	17990
200	9250	6002	7002	3992
200	17040	21004	32704	37804
200	15456	20391	19654	18004
200	12000	17014	18914	29914
150	28060	31860	25860	22860
150	20600	20851	20151	21171
150	23754	23754	34954	45954
150	27580	35892	44102	47292
100	108100	118100	125700	129901
100	101123	101123	100923	99923
100	108600	108200	115801	129801
100	107210	108980	108980	112780

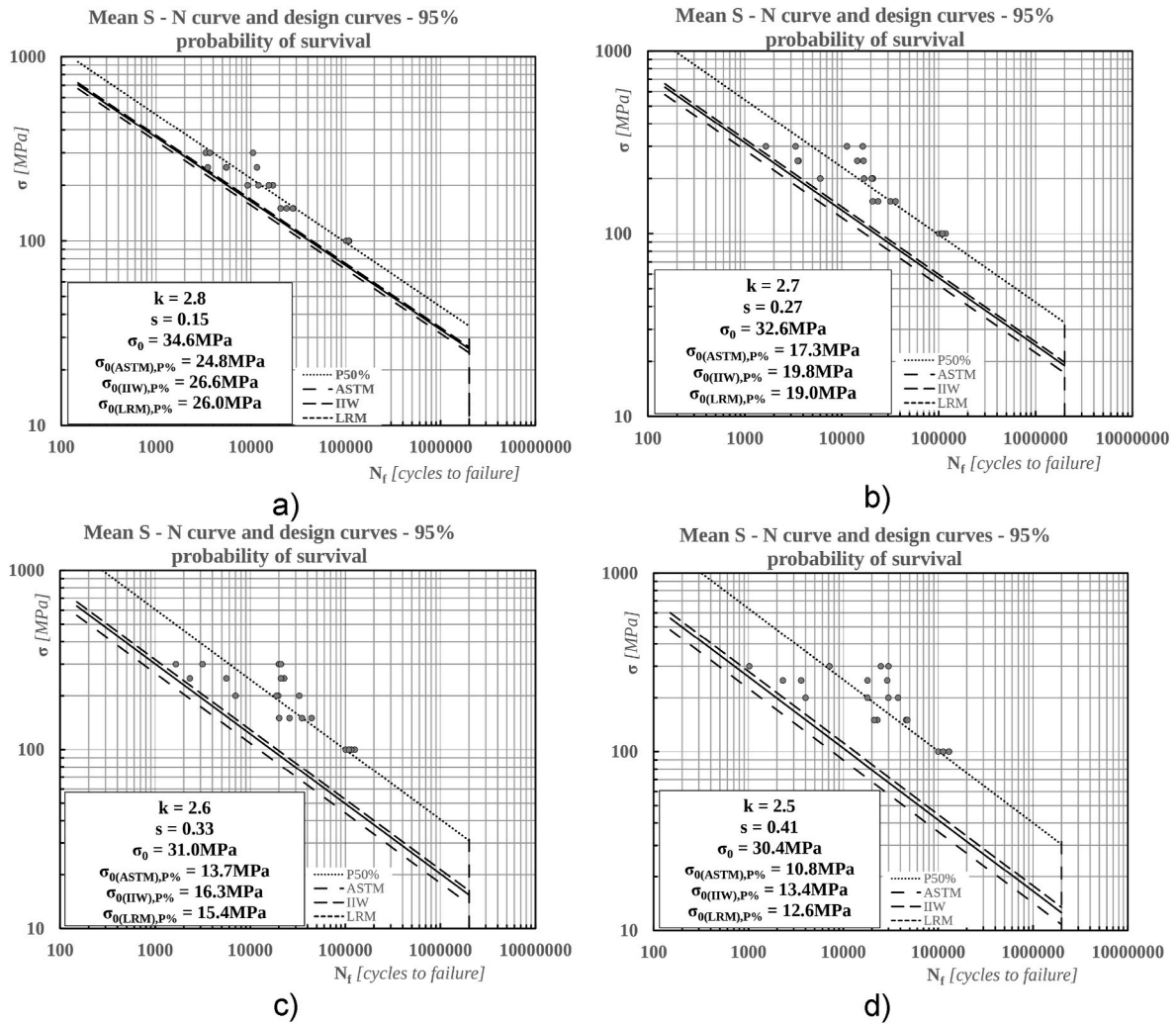


Fig. 6. Graphs representing data from Table 5 a) Mean and design curve for data 1, b) Mean curve and design curve for data 2, c) Mean curve and design curve for data 3, d) Mean curve and design curve for data 4.

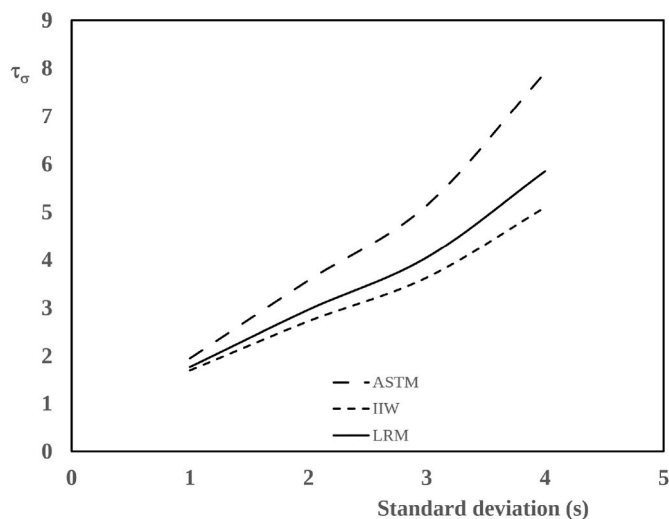


Fig. 7. Change of scatter band with increasing variance.

extent and remains fairly constant as long as the stress range and standard deviation are kept constant.

It should be noted that the analysis considered in this section has not

been adjusted as summarised in Table 3. Because the impact of this on the size of the scatter band generated by the IIW method is not more than 2% [26], this will have negligible effect on the size of the scatter band in comparison with the other approaches.

Table 8 summarises the impacts of the statistical characteristics of fatigue data sets on the sizes of the scatter bands generated using the aforementioned approaches. The spread and the inverse slope are the deterministic parameters that greatly impact the fatigue design curve using the standardised approaches described in this study.

5.2. Verification of approaches using fatigue data sets from literature

The approaches were also tested on real fatigue data sets from the literature. Though it is a challenge to find fatigue data sets that have statistical characteristics that change in defined patterns, it is essential to see how these approaches are impacted by the varied statistical properties of experimental fatigue data. Table 9 summarises some of the fatigue data sets obtained from the literature that were used to compare these approaches.

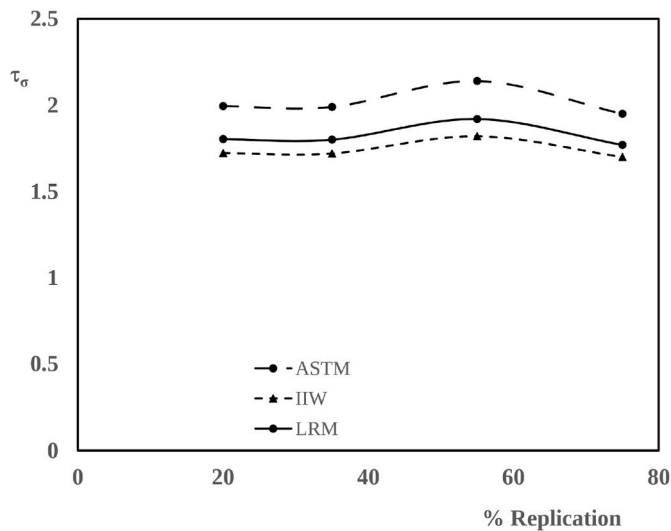
5.2.1. Impact on scatter band size with increasing inverse slope

In as much as the variance and sample set is not constant, the sizes of the scatter band reduce and tend to arrive at a common size for high values of inverse slopes. At low values of inverse slope, the impact on the scatter band is rigorous, though this could be dependent on the other

Table 6

Variatied replication level of theoretical fatigue data with constant variance, sample set and inverse slope.

R = 20%		R = 35%		R = 55%		R = 75%	
σ (MPa)	N_f (cycles)	σ (MPa)	N_f (cycles)	σ (MPa)	N_f (cycles)	σ (MPa)	N_f (cycles)
300	3650	300	3650	300	3650	300	3650
290	3345	290	3345	300	3345	300	3345
280	3685	280	3685	280	3685	300	3685
270	10505	270	10505	280	10505	300	10505
260	5498	260	5498	250	5498	250	5498
250	11560	250	11560	250	11560	250	11560
240	3510	240	3510	230	3510	250	3510
230	5500	240	5500	230	5500	250	5500
220	9250	220	9250	200	9250	200	9250
210	17040	220	17040	200	17040	200	17040
200	15456	200	15456	180	15456	200	15456
190	12000	200	12000	180	12000	200	12000
180	28060	180	28060	150	28060	150	28060
180	20600	180	20600	150	20600	150	20600
150	23754	150	23754	130	23754	150	23754
150	27580	150	27580	130	27580	150	27580
130	108100	130	108100	100	108100	100	108100
130	101123	130	101123	100	101123	100	101123
100	108600	100	108600	100	108600	100	108600
100	107210	100	107210	100	107210	100	107210

**Fig. 8.** Change in the size of scatter band with percentage replication.

statistical properties that characterise the data set. The scatter band from the ASTM approach is always bigger while those from the IIW and LRM approaches are similar as illustrated in Fig. 11.

5.2.2. Impact on scatter band with increasing variance

As summarised in Table 9, the sizes of the scatter band for all data sets from literature fall in the range between 1 and 3. As the variance increases, the sizes of the scatter bands increase and the ratio of each scatter band to the other remains fairly constant. The ASTM remains the approach that produces the largest scatter band. Fig. 11 illustrates the scatter bands of the data summarised in Table 9.

5.2.3. Impact of sample set and replication percentage on size of scatter band

No noticeable effect was observed when the data set was increased. However, the sizes of the scatter bands were dependent on the slope and variance of the fatigue data sets. This same effect was observed with the percentage replication as both of these properties of fatigue data only increase the accuracy and reliability of the estimated statistical properties of the data set.

The graphs in Fig. 12 compare the S–N curves in Refs. [39,40]. As the variance increases from 0.21 to about 0.42 the size of the scatter bands reduces. However, the inverse slope increases from 2.65 to 24.87 and the endurance limits also increase for these sets of fatigue data. It is difficult to attribute the change in the scatter bands to a change in any of the statistical properties because of their interdependence. This illustrates one of the challenges of using experimental data sets without defined patterns in the statistical properties to compare the impacts of the approaches reviewed in this paper.

6. Discussion

A sound understanding of the statistical behaviour of fatigue properties is essential for design in the industry. To estimate the probability of survivals of materials, a suitable probability distribution function that is well suited to the data set is essential. While Weibull two- and three-parameter, log-normal, extreme maximum value, and smallest extreme value are well established distributions extensively used with fatigue data sets, a priori knowledge of these distributions of the data is prerequisite. This might be tricky for use on new data sets for new materials and approaches described in this paper provide an alternative approach to design with less knowledge of which distribution fits the data well. However, some of the cutting-edge models, for example the 9 parameters Weibull regression model [41], that can be estimated by maximum likelihood and also by non-linear regression analyses use a regression model that includes consideration of mean stress effects.

Evidently, whenever a fatigue limit exists [42] the plots of fatigue life versus stress often exhibit curvature at lower stress levels. In addition to this, the variance of the fatigue life decreases as the number of stress levels increase. Ideally, the standard deviation should be modelled as a function of the stress levels for which an endurance limit can be estimated at those stress levels [43]. This is the model behind the fatigue limit approach of constructing the design curves. This is quite straight forward compared to the approaches described herein where the fatigue limit may not be known in advance and is particularly useful when considering endurance limits rather than fatigue limits. However, the variability in design curves could be expected as a consequence of the fatigue limit being dependent on the material's structural properties which may vary from specimen to specimen. This limits the accuracy of the design curves generated using this approach to the factors that determine the fatigue limit of the material in question.

In as much as the Maximum Likelihood Estimate methodology is the preferred method of analysis of censored and uncensored data using the

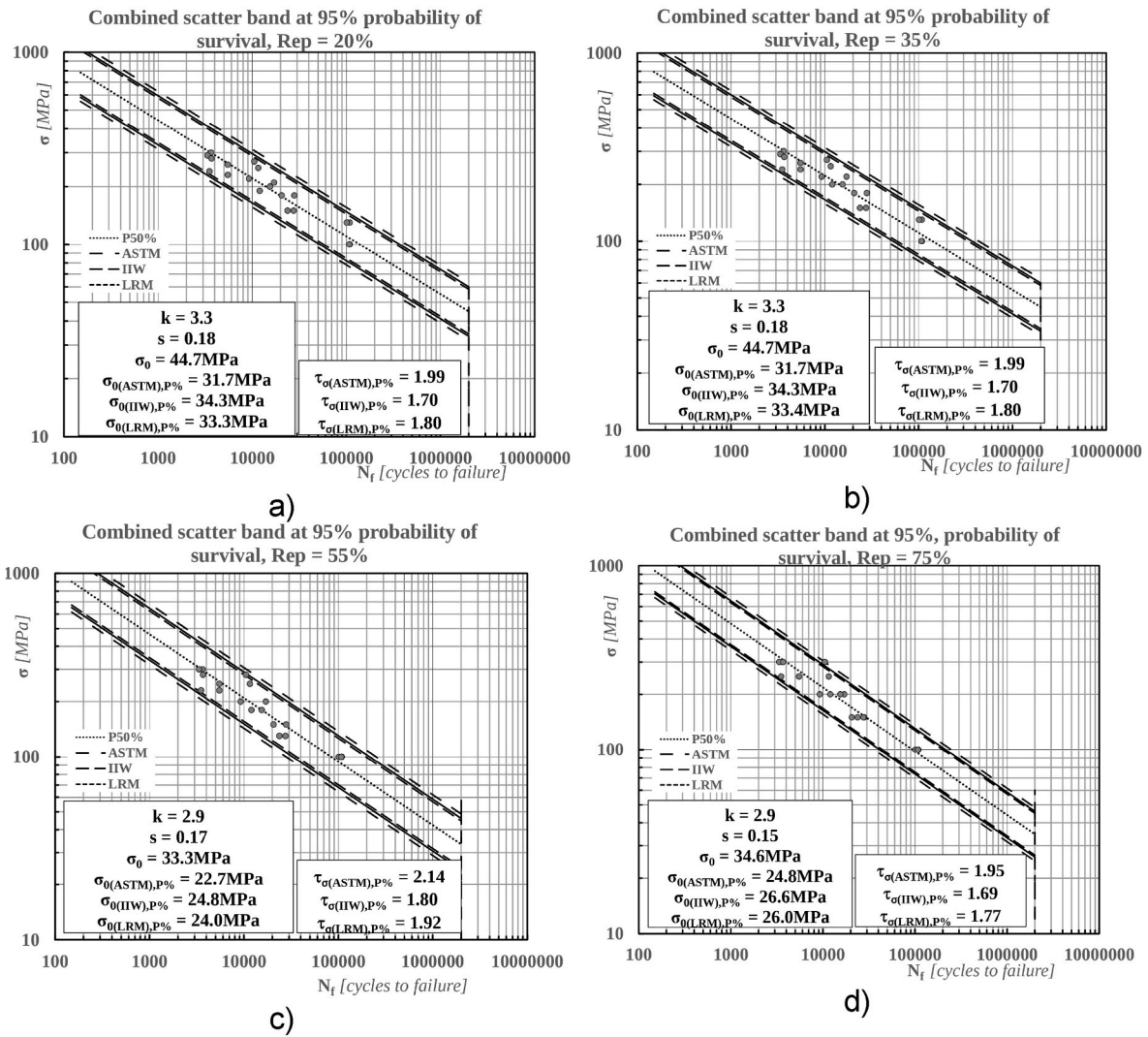


Fig. 9. Varied replication level of theoretical fatigue data with constant variance, sample set and inverse slope and spread. a) 20%, b) 35%, c) 55% and d) 75%.

Table 7

Theoretical fatigue data with varied degrees of freedom with constant percentage replication and variance.

n = 6		n = 8		n = 12	
σ (MPa)	N_f (cycles)	σ (MPa)	N_f (cycles)	σ (MPa)	N_f (cycles)
290	4682	290	2912	290	1956
270	56245	280	45258	280	17256
250	123254	270	60254	270	36124
230	358222	250	135246	260	49123
210	1235452	230	452132	255	65123
210	1352658	220	985254	250	85568
		210	1113256	240	92624
		210	1292583	230	109253
				220	852358
				215	1052581
				210	1088653
				210	1366875

staircase method to generate experimental results [34], this method still has some limitations and consequently, there does not exist a more preferred method to post process experimental fatigue censored data and the approach used by any organisation is a decision of choice. While some make use of safety factors, others choose a probabilistic approach to which this study owes its relevance. There are other cutting-edge

approaches that use statistical considerations, some of which are the one-sided approximate Owen lower limit as well as the Weibull approaches which all agree with the approaches described in this study. Other organisations use software behind which the concepts are similar. This buttresses the fact that no method is more accurate than the other, however when cost, sustainability and critical application is put into perspective, some methods tend to be more favourable than others.

The approaches have assumed the fatigue data to have a linear relationship and there exist quite a few linear models [15] which differ in their approach to estimate the parameters of the mean S-N curve. Linearity is not usually the case; however, fatigue tests are usually carried out a stress levels where the S-N will be linear. This a priori knowledge is dependent on the researcher and may not be assessable for new materials. However, the linear relation consideration has enabled the impacts of distributions that are symmetrical or tend to approximate to symmetric distributions under particular considerations.

Furthermore, fatigue data has been censored by ignoring runouts or suspended tests. This is the simplified approach to runouts and results in the mean curve being biased slightly in the long-life regime [15]. The ASTM method advises against censoring fatigue data, however, there is not much difference between the design curves with censored and uncensored data. Though this is insignificant for low spreads, it becomes quite observant in situations with very low stress levels where the spread in fatigue life is very significant. If the runouts are treated as failures, as

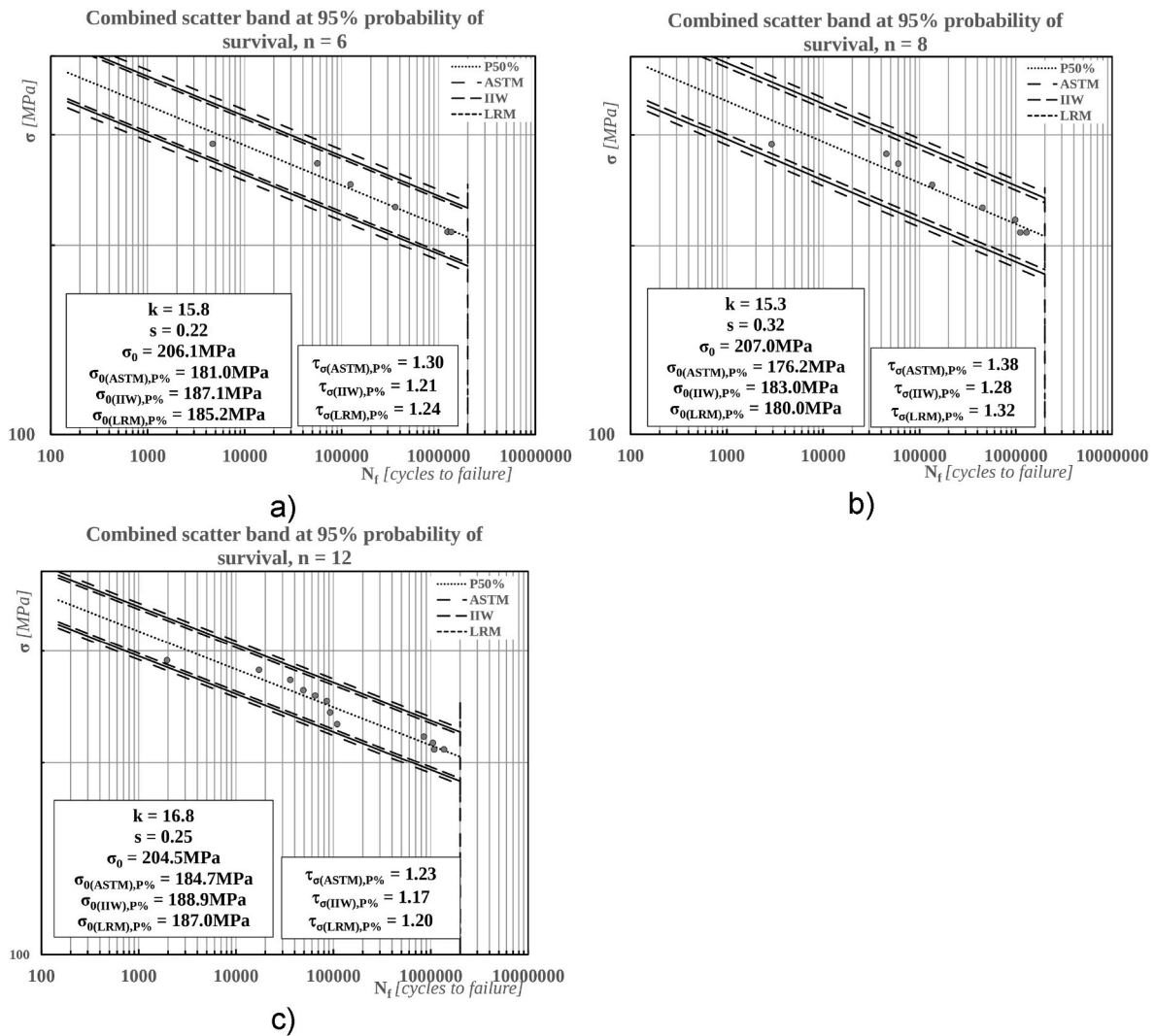


Fig. 10. Scatter bands and design stresses for varied magnitude of sample set a) $n = 6$, b) $n = 8$, and c) $n = 12$.

Table 8

Summary of the changes in size of scatter band with the characteristics of fatigue data.

Parameter	Impact on scatter bands
1) Inverse slope	<ul style="list-style-type: none"> ➤ Scatter bands decrease with increase inverse slope ➤ Scatter bands converge for inverse slopes ≥ 20.
2) Spread (variance)	<ul style="list-style-type: none"> ➤ Scatter bands increases ➤ For spread $\leq 2s$, scatter bands are similar ➤ No change in size of scatter bands
3) Replication	<ul style="list-style-type: none"> ➤ Dependent on the spread at each stress amplitude ➤ No change in the size of scatter bands.
4) Sample size	<ul style="list-style-type: none"> ➤ Depends on the overall spread of the data.

mentioned in Ref. [15], the bias would increase further. In such a case, this will tilt the mean curve towards more conservativeness. Other methods consider runouts as failures if they occur at stress levels above the reference stress. Maximum likelihood procedures consider runouts as part of the data to be analysed while iterative least squares procedures are another option even though these approaches haven proven to be quite rigorous.

The use of prediction limits as the fatigue design curve in the ASTM approach has shown that it is very conservative. The approach detailed by the IIW is less conservative and differs from the LRM approach by not more than 5%. The adjustment in the scatter bands as described by the

IIW approach makes great use of the statistical characteristics of the data set when compared with the LRM approach. However, the LRM approach is very easy and straight forward to use even though it is less sensitive to outliers and is applicable for all data. The LRM approach is not restricted by the sample sets when compared with the other models especially the ASTM approach.

More so, the LRM approach assumes data to be independent of each other. The fatigue life at high stress levels does not change at the same rate as at low stress levels. The fatigue life result for a stress level determines the next stress level during testing up to the vicinity of the endurance limit, yet the variance of this fatigue life increases along the S-N curve in reality.

7. Conclusions

By considering the assumptions outlined in section 3.1, this paper undertakes a thorough comparison and evaluation of the fatigue assessment procedures recommended by the ASTM, IIW, and LRM. The results clearly indicate that all three approaches lead to the attainment of a safe design methodology. Building upon the detailed analysis conducted in this study, which covers uniaxial S-N curves derived from both virtual fatigue data sets and some existing fatigue data sets from the literature, the following conclusions can be drawn.

Table 9
Summary of fatigue data sets from literature with sample set, variances and inverse slope parameters determined.

Source	Description (fig/table)	Sample set, n	Inverse slope, k	Variance, s^2	$\tau_{\sigma(ASM)}$	$\tau_{\sigma(IIW)}$	$\tau_{\sigma(LM)}$
[44]	Fig. 1	5	22.01	0.26	1.30	1.19	1.22
[44]	Fig. 2	4	41.49	0.29	1.24	1.143	1.14
[44]	Fig. 3	5	24.87	0.42	1.46	1.28	1.33
[44]	Fig. 4	4	33.88	0.23	1.24	1.145	1.14
[44]	Fig. 9, Dry	6	17.82	0.09	1.09	1.06	1.07
[44]	Fig. 9, Aged	8	16.48	0.29	1.31	1.22	1.27
[45]	Fig. 11	16	16.22	0.16	1.14	1.10	1.12
[46]	Fig. 5	11	6.97	0.14	1.32	1.24	1.27
[14]	Tab 4.2	12	26.5	0.49	1.29	1.21	1.25
[47]	Fig. 5, Plain specimens	7	7.71	0.13	1.31	1.21	1.26
[47]	Fig. 5, Blunt U-notch	8	3.50	0.08	1.43	1.29	1.36
[47]	Fig. 5, Sharp U-notch	7	3.40	0.12	1.78	1.50	1.64
[47]	Fig. 5, Sharp V-notch	9	2.65	0.21	3.2	2.33	2.76
[48]	Fig. 2a), $R = 0$	6	7.25	0.31	2.22	1.73	1.92
[48]	Fig. 2b)	6	18.45	0.13	1.14	1.10	1.11
[48]	Fig. 3a), $R = -1$	6	9.85	0.34	1.89	1.55	1.69
[40]	Fig. 5, TMM	4	11.51	0.26	2.06	1.57	1.55
[40]	Fig. 5, Exp.	4	17.32	0.25	1.58	1.33	1.32
[40]	Fig. 6, Exp.	5	17.83	0.37	1.59	1.36	1.42
[40]	Fig. 6, TMM	5	3.69	0.003	1.02	1.01	1.01
[38]	Fig. 6c), $R = 0.1$	8	4.38	0.24	2.34	1.84	2.09
[38]	Fig. 6c), $R = -1$	6	6.45	0.24	2.00	1.61	1.77
[38]	Fig. 6e), $R = -1$	11	10.77	0.40	1.68	1.50	1.58

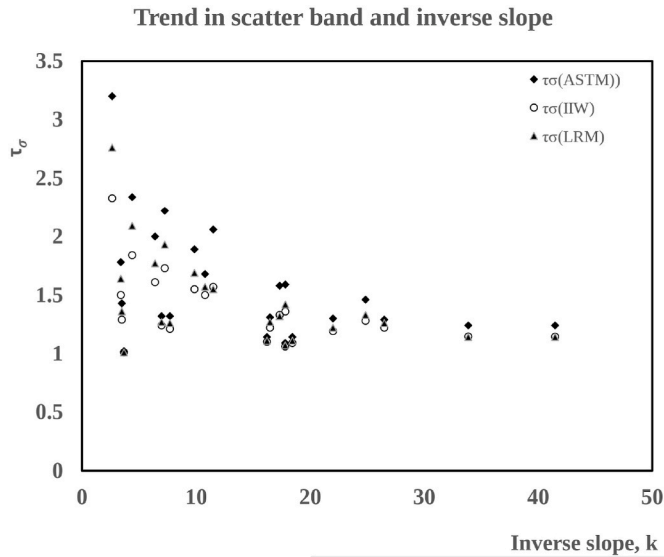


Fig. 11. Trends in scatter band with increasing inverse slope of selected fatigue datasets from literature.

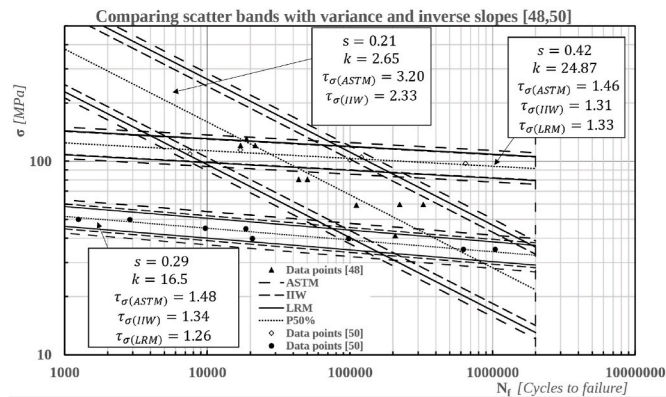


Fig. 12. Comparing scatter bands of ASTM, IIW and LRM of fatigue data sets from literature with changing variance, inverse slope and sample set.

- The IIW approach is the most non-conservative approach and would reduce any chance of overdesign when compared to the other approaches. This would be very applicable for sustainable components. The design curve in this case is dependent on the characteristics of the data, in particular the sample size and its spread. The use of a student's t-distribution makes the case for application due to the inherent null hypothesis with future populations. The critical values for each probability can easily be calculated or read from statistical tables which are readily available in the literature.
- Sensitivity of the design approach to the spread of the fatigue data was observed more in the ASTM approach. This method is therefore very conservative and would substitute for approaches with very large factors of safety or in designing critical parts of components.
- Fatigue data with very little spread will not be affected greatly by the approach used to calculate the design curve. However, if very large probabilities of survival are used for design, care should be taken on which approach is recommended.
- The simplest to use approach is the linear regression method and the empirical constants corresponding to sample sizes are defined in the ASTM standards for fatigue distributions with assumed shapes. This approach is not limited by the sample size of the data set.

CRedit authorship contribution statement

Elvis Kufoin: Writing – original draft, Formal analysis, Data curation. **Luca Susmel:** Writing – review & editing, Supervision, Project administration, Methodology, Funding acquisition, Conceptualization.

Declaration of competing interest

The Authors declare that:

- 1) there exists no conflict of interest.
- 2) no funding was received for this work.
- 3) no research ethics issues are involved.
- 4) the work described has not been published previously.
- 5) it is not under consideration for publication elsewhere.
- 6) if accepted, it will not be published elsewhere in the same form, in English or in any other language, without the written consent of the Publisher.

Data availability

Data will be made available on request.

References

- [1] R. I Stephens, A. Fatemi, R. R Stepens, H. O Fuchs, *Metal Fatigue in Engineering*, second ed., Second, John Wiley & Sons, New York, 2001.
- [2] A. Tridello, C. Boursier Niutta, F. Berto, M.M. Tedesco, S. Plano, D. Gabellone, D. S. Paolino, Design against fatigue failures: lower bound P-S-N curves estimation and influence of runout data, *Int. J. Fatig.* 162 (2022) 106934, <https://doi.org/10.1016/j.ijfatigue.2022.106934>.
- [3] S.K. Paul, A. Nayak Majila, D.C. Fernando, Statistical analysis of uniaxial tensile and fatigue data of Ti-685 alloy at different temperatures, *Forces in Mechanics* 4 (2021) 100046, <https://doi.org/10.1016/j.finmec.2021.100046>.
- [4] A. Tridello, D.S. Paolino, LCF-HCF strain-life model: statistical distribution and design curves based on the maximum likelihood principle, *Fatig. Fract. Eng. Mater. Struct.* 46 (2023) 2168–2179, <https://doi.org/10.1111/ffe.13990>.
- [5] ASTM E739-10, Standard Practise for Statistical Analysis of Linear or Linearized Stress-Life (S-N) and Strain-Life (ε-N) Fatigue Data, ASTM, 2010, pp. 1–7, <https://doi.org/10.1520/E0739-23.2>.
- [6] E. Castillo, A. Fernández-Canteli, H. Pinto, M. Lopez-Aenlle, A general regression model for statistical analysis of strain-life fatigue data, *Mater. Lett.* 62 (21–22) (2008) 3636–3642. <https://doi-org.sheffield.idm.oclc.org/10.1016/j.matlet.2008.04.015>.
- [7] D.S. Paolino, A. Tridello, G. Chiandussi, M. Rossetto, S-N curves in the very-high-cycle fatigue regime: statistical modeling based on the hydrogen embrittlement consideration, *Fatig. Fract. Eng. Mater. Struct.* 39 (2016) 1319–1336, <https://doi.org/10.1111/ffe.12431>.
- [8] A. Arcari, N. Apetre, N. Dowling, M. Meischel, S. Stanzl-Tschegg, N. Iyyer, N. Phan, Variable amplitude fatigue life in VHCF and probabilistic life predictions, *Procedia Eng.* 114 (2015) 574–582, <https://doi.org/10.1016/j.proeng.2015.08.107>.
- [9] J.P. Park, S. Mohanty, C.B. Bahn, S. Majumdar, K. Natesan, Weibull and bootstrapped data-analytics framework for fatigue life prognosis of the pressurized water nuclear reactor component under harsh reactor coolant environment, *J Nondestruct Eval Diagn Progn Eng Syst* 3 (2020) 332–370, <https://doi.org/10.1115/1.4045162>.
- [10] J. Chen, Y. Liu, Fatigue modeling using neural networks: a comprehensive review, *Fatig. Fract. Eng. Mater. Struct.* 45 (2022) 945–979, <https://doi.org/10.1111/ffe.13640>.
- [11] M.S. Nashed, M.S. Mohamed, O.T. Shady, J. Renno, Using probabilistic neural networks for modeling metal fatigue and random vibration in process pipework, *Fatig. Fract. Eng. Mater. Struct.* 45 (2022) 1227–1242, <https://doi.org/10.1111/ffe.13660>.
- [12] R.E. Little, J.C. Ekvall, *Statistical Analysis of Fatigue Data*, ASTM STP 744, American Society for Testing and Materials, 1981.
- [13] C.L. Shen, P.H. Wirsching, G.T. Cashman, Design curve to characterize fatigue strength, *Journal of Engineering Materials and Technology*, Transactions of the ASME 118 (1996) 535–541, <https://doi.org/10.1115/1.2805953>.
- [14] Y. Lee, J. Pan, R. B Hathaway, M. E Barkey, *Fatigue Testing and Analysis: Theory and Practice*, Elsevier Butterworth-Heinemann., Amsterdam; Boston, 2005.
- [15] R.C. Rice, B.C. Laboratories, *Fatigue Data Analysis*, ASM Handbook Committee, 2015.
- [16] R.I. Stephens, A. Fatemi, R.R. Stephens, Henry O. Fuchs, *Metal Fatigue in Engineering*, second ed., John Wiley & Sons, New York, 2000.
- [17] C.C. Engler-Pinto Jr., J. V Lasecki, R.J. Frisch Sr., M.A. DeJack, J.E. Allison, R. J. Frisch Michael A DeJack, *Statistical Approaches Applied to Fatigue Test Data Analysis Statistical Approaches Applied to Fatigue Test Data an*, 2005.
- [18] N.E. Dowling, Estimating fatigue life, in: *Fatigue and Fracture*, ASM International, 1996, pp. 250–262, <https://doi.org/10.31399/asm.hb.v19.a0002365>.
- [19] D.E. Norman, *Mechanical Behavior of Materials : Engineering Methods for Deformation, Fracture, and Fatigue*, first ed., Prentice Hall International , INC, Englewood Cliffs, New Jersey ; London, England, 1993.
- [20] C. R Schneider, S. J Maddox, *BEST PRACTICE GUIDE ON STATISTICAL ANALYSIS OF FATIGUE DATA*, 2003.
- [21] G.J. Hahn, Statistical methods for creep, fatigue and fracture data analysis, *Journal of Engineering Materials and Technology*, Transactions of the ASME 101 (1979) 344–348, <https://doi.org/10.1115/1.3443700>.
- [22] J.F. Barbosa, J.A. Correia, R. Freire, S.-P. Zhu, A. De Jesus, Probabilistic S-N fields based on statistical distributions applied to metallic and composite materials, *Adv. Mech. Eng.* 11 (8) (2019) 1–22, <https://doi.org/10.1177/1687814019870395>.
- [23] D. Leonetti, J. Maljaars, H.H. Bert Snijder, Fitting fatigue test data with a novel S-N curve using frequentist and Bayesian inference, *Int. J. Fatig.* 105 (2017) 128–143, <https://doi.org/10.1016/j.ijfatigue.2017.08.024>.
- [24] P.H. Wirsching, *Statistical Summaries of Fatigue Data for Design Purposes*, NASA Contractor Reports, 1983.
- [25] R. Khelif, A. Chateaufneuf, K. Chaoui, Statistical analysis of HDPE fatigue lifetime, *Meccanica* 43 (2008) 567–576, <https://doi.org/10.1007/s11012-008-9133-7>.
- [26] F. Lefebvre, I. Huthier, G. Parmentier, M. Huthier, Document XIII-2807-19 BEST PRACTICE GUIDELINE for STATISTICAL ANALYSES of FATIGUE RESULTS, 2019.
- [27] S.M. Marco, H.E. Frankel, M.N. Torrey, C.A. Moyer, A guide for fatigue testing and the statistical analysis of fatigue data, *Am. J. Orthod.* 51 (1963) 318, [https://doi.org/10.1016/0002-9416\(65\)90116-8](https://doi.org/10.1016/0002-9416(65)90116-8).
- [28] C. Johnston, “TWI Ltd,” TWI Ltd, Granta Park Great Abington, 25 JUNE, Cambridge, 2017 [Online]. Available: <https://www.twi-global.com/technical-knowledge/published-papers/statistical-analysis-of-fatigue-test-data#ref4>. (Accessed 25 March 2022).
- [29] W. J Youden, L. Tanner, S. Collier, H.F. Dodge, R.J. Hader, G.J. Lieberman, *ASTM MANUAL ON FITTING STRAIGHT LINES*, Prentice Hall Inc., Englewood Cliffs, N.J., 1959.
- [30] STP46393S, *ASTM Manual on Fitting Straight Lines*, ASTM Manual on Fitting Straight Lines, vol. 1, 2009, pp. 1–28, <https://doi.org/10.1520/stp46393s>.
- [31] A. Kurek, Using fatigue characteristics to analyse test results for 16Mo3 steel under tension-compression and oscillatory bending conditions, *Materials* 13 (5) (2020), <https://doi.org/10.3390/ma13051197>.
- [32] R.E. Little, E.H. Jebe, *Statistical Design of Fatigue Experiments*, Applied Science Publishers., London, 1975.
- [33] R.D. Pollak, A.N. Palazotto, A comparison of maximum likelihood models for fatigue strength characterization in materials exhibiting a fatigue limit, *Probabilist. Eng. Mech.* 24 (2009) 236–241, <https://doi.org/10.1016/j.probgmech.2008.06.006>.
- [34] C.C. Engler-Pinto, J.V. Lasecki, R.J. Frisch Sr., M.A. DeJack, J.E. Allison, *Statistical Approaches Applied to Fatigue Test Data Analysis*, SAE International, 2005. <https://www.jstor.org/stable/44718917>.
- [35] K. Störzel, J. Baumgartner, Statistical evaluation of fatigue tests using maximum likelihood, *Mater. Test.* 63 (2021) 714–720, <https://doi.org/10.1515/mt-2020-0116>.
- [36] M. Pasalic, F. Rustempasic, S. Iyengar, S. Melin, E. Noah, Fatigue testing and microstructural characterization of tungsten heavy alloy Densimet 185, *Int. J. Refract. Metals Hard Mater.* 42 (2014) 163–168, <https://doi.org/10.1016/j.jrhm.2013.09.001>.
- [37] ASTM E3080, *Standard Practice for Regression Analysis with a Single Predictor Variable 1*, ASTM, 2019, pp. 1–20, <https://doi.org/10.1520/E3080-19.2>.
- [38] L. Susmel, D.G. Hattinng, M.N. James, R. Tovo, Multiaxial fatigue assessment of friction stir welded tubular joints of Al 6082-T6, *Int. J. Fatig.* 101 (2017) 282–296, <https://doi.org/10.1016/j.ijfatigue.2016.08.010>.
- [39] L. D’Angelo, A. Nussbaumer, Estimation of fatigue S-N curves of welded joints using advanced probabilistic approach, *Int. J. Fatig.* 97 (2017) 98–113, <https://doi.org/10.1016/j.ijfatigue.2016.12.032>.
- [40] M.R. Rahim, S. Schmauder, Y.H. Manurung, P. Binkele, M.I. Ahmad, K. Dogahe, Cycle Number Estimation Method on Fatigue Crack Initiation Using Voronoi Tessellation and the Mura Model, *ASM International*, 2023, <https://doi.org/10.1007/s11668-023-01603-0>.
- [41] E. Castillo, A. Fernández-Canteli, R. Koller, M.L. Ruiz-Ripoll, A. García, A statistical fatigue model covering the tension and compression Wöhler fields, *Probabilist. Eng. Mech.* 24 (2009) 199–209, <https://doi.org/10.1016/j.probgmech.2008.06.003>.
- [42] O. Kaleva, H. Orelma, Statistical properties of the model parameters in the continuum approach to high-cycle fatigue, *Probabilist. Eng. Mech.* 63 (2021), <https://doi.org/10.1016/j.probgmech.2021.103117>.
- [43] R.D. Pollak, A.N. Palazotto, A comparison of maximum likelihood models for fatigue strength characterization in materials exhibiting a fatigue limit, *Probabilist. Eng. Mech.* 24 (2009) 236–241, <https://doi.org/10.1016/j.probgmech.2008.06.006>.
- [44] Q.C. Bourgogne, V. Bouchart, P. Chevrier, Prediction of the Wöhler curves of short fibre reinforced composites considering temperature and water absorption, *Mater. Today Commun.* 33 (2022) 104655, <https://doi.org/10.1016/j.mtcomm.2022.104655>.
- [45] L. Jegou, Y. Marco, V. Le Saux, S. Calloch, Fast prediction of the Wöhler curve from heat build-up measurements on Short Fiber Reinforced Plastic, *Int. J. Fatig.* 47 (2013) 259–267, <https://doi.org/10.1016/j.ijfatigue.2012.09.007>.
- [46] O. Kaleva, H. Orelma, D. Petukhov, Parameter estimation of a high-cycle fatigue model combining the Ottosen-Stenström-Ristinmaa approach and Lemaitre-Chaboche damage rule, *Int. J. Fatig.* 147 (2021), <https://doi.org/10.1016/j.ijfatigue.2021.106153>.
- [47] R. Louks, L. Susmel, The linear-elastic Theory of Critical Distances to estimate high-cycle fatigue strength of notched metallic materials at elevated temperatures, *Fatig. Fract. Eng. Mater. Struct.* 38 (2015) 629–640, <https://doi.org/10.1111/ffe.12273>.
- [48] A. Niesiony, M. Böhm, Fatigue life of S355JR steel under uniaxial constant amplitude and random loading conditions, *Mater. Sci.* 55 (2020) 514–521, <https://doi.org/10.1007/s11003-020-00333-0>.